Florida International University
FIU Digital Commons

FIU Electronic Theses and Dissertations | University Graduate School

7-26-1996

Laser cooling of a metastable argon atomic beam

Carlos A. Avila
Florida International University

DOI: 10.25148/etd.FI14032375
Follow this and additional works at: https://digitalcommons.fiu.edu/etd

 Part of the Physics Commons

Recommended Citation
Avila, Carlos A., "Laser cooling of a metastable argon atomic beam" (1996). *FIU Electronic Theses and Dissertations*. 1342.
https://digitalcommons.fiu.edu/etd/1342

This work is brought to you for free and open access by the University Graduate School at FIU Digital Commons. It has been accepted for inclusion in FIU Electronic Theses and Dissertations by an authorized administrator of FIU Digital Commons. For more information, please contact dcc@fiu.edu.

FLORIDA INTERNATIONAL UNIVERSITY

Miami, Florida

LASER COOLING OF A METASTABLE ARGON ATOMIC BEAM

A thesis submitted in partial satisfaction of the

requirements for the degree of

MASTER OF SCIENCE

IN

PHYSICS

by

Carlos A. Avila

1996

To: Arthur W. Herriott
College of Arts and Sciences

This thesis, written by Carlos A. Avila, and entitled LASER COOLING OF A METASTABLE ARGON ATOMIC BEAM, having been approved in respect to style and intellectual content, is referred to you for judgement.

We have read this thesis and recommend that it be approved.

Dr. John Landrum

Dr. Yifu Zhu

Dr. Stephan Mintz

Dr. Kenneth Hardy, Major Professor

Date of Defense: July 26, 1996

The thesis of Carlos A. Avila is approved.

Dean Arthur W. Herriott
College of Arts and Sciences

Dr. Richard L. Campbell
Dean of Graduate Studies

Florida International University, 1996

To my family

ACKNOWLEDGEMENTS

First, I wish to thank the members of my committee for their helpful comments. I would also like to thank my co-workers for their help and friendship: G. Hernandez, G. B. Ramos, M. Faxas, L. Simons, J.C. Catala and I. Suarez. Let me also thank the Physics Department faculty and staff for their instruction and encouragement. I am forever grateful to Carlos Orta, Norman Huang, Ofelia Adan-Fernandez and Hiddy Doren for always lending a helping hand.

I would like to give special thanks to Dr. Kenneth Hardy for his patience, unwavering support, constant encouragement and, most of all, his faith in me.

ABSTRACT OF THE THESIS

LASER COOLING OF A METASTABLE ARGON ATOMIC BEAM

by

Carlos A. Avila

Florida International University, 1996

Miami, Florida

Professor Kenneth Hardy, Major Professor

A production of low velocity and monoenergetic atomic beams would increase the resolution in spectroscopic studies and many other experiments in atomic physics. Laser Cooling uses the radiation pressure to decelerate and cool atoms. The effusing from a glow discharge metastable argon atomic beam is affected by a counterpropagating laser light tuned to the cycling transition in argon. The Zeeman shift caused by a spatially varying magnetic field compensates for the changing Doppler shift that takes the atoms out of resonance as they decelerated. Deceleration and velocity bunching of atoms to a final velocity that depends on the detuning of the laser relative to a frequency of the transition have been observed. Time-of-Flight (TOF) spectroscopy is used to examine the velocity distribution of the cooled atomic beam. These TOF studies of the laser cooled atomic beam demonstrate the utility of laser deceleration for atomic-beam "velocity selection".

TABLE OF CONTENTS

LIST OF TABLES

TABLES **PAGES**

LIST OF FIGURES

Chapter I - INTRODUCTION

Thermal motion of atoms imposes a limit to many laboratory measurements in atomic physics. The average kinetic energy of this motion is directly proportional to absolute temperature and thus can never be eliminated except at the unattainable temperature of absolute zero. The high velocity of free atoms associated with the thermal motion (typically 500 m/s at ordinary temperature), together with the velocity distribution of the atoms, has produced the ultimate limitation on a variety of high precision measurements.

The precision of ultrahigh resolution spectroscopy is limited by the motion of the atoms being observed. The frequencies associated with transitions between atomic energy levels are shifted and spread. There are techniques for observation of optical spectra that are nearly free of the first-order Doppler effect,[1-5] but the second-order Doppler effect, associated with the relativistic time dilation, is still present. The small observation time available when one looks at rapidly moving atoms causes the broadening of the spectral line ($\Delta\nu\Delta\tau\approx\hbar$). A sample consisting of low velocity or mono-velocity atoms would provide a substantial improvement in spectroscopic resolution.

Detailed studies of collision phenomena, which require precise knowledge of the initial velocities, are similarly hampered by the randomness of thermal motion. Neither the direction nor the magnitude of the relative velocity of two colliding atoms is well defined when velocities are distributed thermally. Velocity selection using a mechanical chopper leads to a well-defined velocity, but selection is inefficient in that most of the atoms in the atomic beam are not used. Velocity compression techniques can yield high beam flux with relative well-defined velocity, but low velocities are not attainable.[6] A laser-cooled atomic beam makes efficient use of the atoms, and achieves a narrow and selectable velocity. Laser-cooling has the additional advantage of being able to place all the atoms in a single internal quantum state and at low velocities.

Another application for a collection of low velocity and/or mono-velocity atoms would be as an ideal target for a variety of low energy and/or high energy-resolution scattering experiments, chemical reaction studies, or surface studies. In addition, many other kinds of experiments with atomic beams, such as studies of the deflection of atoms by light,[7] sensitive beam deflection experiments for the study of quantum statistics in optical absorption and emission[8] and searches for intrinsic electric dipole moments,[9] would benefit from reduction of the thermal

motion of the atoms and production of monoenergetic atomic beams.

Some interesting collision processes become important only at low velocities. When the velocity of the collision partners is low enough, their corresponding de Broglie wavelength becomes long compared to the range of their interaction potential. Under these conditions the collision partners cannot be treated as if their had a classical trajectory, and the collision is dominated by quantum effects.

Bose-Einstein condensation (BEC) only occurs when atoms are so cold that the thermal de Broglie wavelength becomes larger than the mean spacing between atoms and their quantum nature becomes predominant. For a gas of particles with mass m at temperature T, the de Broglie wavelength λ equals $h/(2\pi m\kappa T)^{1/2}$. Although there are profound differences between fermions and bosons on the microscopic quantum level, the quantum statistics of atoms has never predicted any observable difference to the collective macroscopic properties of a real gas sample. The most striking difference is the prediction, originally by Einstein,[10,11] that a gas of noninteracting bosonic atoms will, below a certain temperature, suddenly develop a macroscopic population in the lowest energy quantum mechanical state. For an ideal gas, this phase transition occurs when the dimensionless phase-space density $\rho=n\lambda^3$ exceeds 2.612 (where

n is the number density). If the density of the gas is low (as is required for a real gas to approximate an ideal gas) this condition requires extremely low temperatures. Recently, BEC was reported in different atomic gases.[12-14] Atoms were laser precooled and then confined in magneto-optical traps. A further evaporative cooling process produced record low temperatures and observation of the condensed state.

To overcome these problems of thermal motion, atomic physicists have pursued two goals, (I) the reduction of the thermal motion (cooling) and (II) the confinement of the atoms by means of electromagnetic fields (trapping). Cooling, carried sufficiently far, eliminates the motional problems, whereas trapping allows for long observation times. Laser cooling was first demonstrated on trapped ions. While ions could first be trapped and then laser-cooled,[15-17] neutral atoms had to be laser cooled before they could be trapped.

When an atom absorbs the energy of a photon, making a transition to a more energetic state, it also absorbs the momentum of the photon and this changes the atomic velocity. Laser cooling uses this velocity change to reduce the thermal motion. The choice of an atom to use in cooling experiments depends on the availability of suitable lasers and the ease of making an intense atomic beam. Also, the spontaneous fluorescence rate must be high enough to

obtain deceleration from thermal to zero velocity in a reasonably sized apparatus.

In this work the laser cooling of an argon atom beam will be discussed. The experiments involve a time-of-flight (TOF) spectroscopy on metastable argon atoms. Chapter II will explain the theory of laser cooling, especially the "Zeeman" cooling. The laser system used in the experiments, the absorption measurements for laser diagnostics, and the optics used to direct the laser beam will be described in Chapter III. In Chapter IV, the atomic beam apparatus is described. The laser hole-burning, the effect of constant magnetic field on the TOF-distribution, and the results of laser cooling experiments will be discussed in Chapter V. Finally Chapter VI will summarize the results of this investigation.

Chapter II - LASER COOLING OF NEUTRAL ATOMS

A. RADIATION PRESSURE

Laser deceleration or cooling of atoms is achieved by directing a photon beam against an atomic beam. The radiation pressure force (also called the scattering force), which has its origin in the momentum transfer between the atoms and a radiation field resonant with an atomic transition, is used to decelerate and/or to cool free neutral atoms.

If the laser is tuned below the frequency of the resonant absorption ν_r, the atom moving toward the laser with velocity v will see the laser frequency Doppler-shifted $\nu=(\nu_r-\delta)(1+v/c)$. When the detuning, δ, compensates for the Doppler shift corresponding to a velocity v ($\delta=\nu_r v/c$), the atom sees the laser frequency resonant $\nu=\nu_r$ and will absorb the photon. The atom will be excited to the high energy state (upon absorption of the photon), and will recoil with a $h\nu/c$ momentum in the direction of the laser beam to conserve the linear momentum. The angular momentum of the photon $\hbar$ is stored in the form of internal motion of the electrons to conserve the angular momentum. As a result of each absorption, the atom's velocity is reduced by $h\nu/Mc$, where M is the mass of the atom. This is the velocity change that is of special interest in laser deceleration or cooling, and although it is very small (typically few cm/s) compared with thermal velocity, multiple absorptions can

produce a large velocity change. For an argon atom this velocity change is about 0.012 m/s per photon absorbed. To stop an argon atom with velocity of 600 m/s, over $5x10^4$ photons must be scattered.

The atom also receives a recoil momentum when it radiates a photon by spontaneous or stimulated emission. For excitation by a plane-wave laser beam, stimulated photons are emitted in the same direction as the incoming photons; so, they cancel the momentum transferred by the absorbed photon. In the spontaneous emission processes, however, photons are emitted in a random direction. The momentum transfer due to spontaneous emission is zero on average, and so the net momentum transfer after absorption followed by spontaneous emission is the momentum transfer of the absorption (Figure 1). After the atom absorbs N photons, the velocity change will be $Nh\nu/Mc$ provided emission is spontaneous. As a result, the atom will receive an accumulated momentum in the direction of the laser beam and be decelerated.

Since the deceleration requires absorption-spontaneous emission cycle, it is limited by the spontaneous fluorescence rate. The maximum attainable deceleration is achieved at very high light intensities ($I>>I_{sat}=\pi hc/\lambda^3\tau$). The saturation intensity, I_{sat}, is the intensity of light that will produce equal rates of stimulated and spontaneous emission, and for most atomic transitions is a few mW/cm^2.

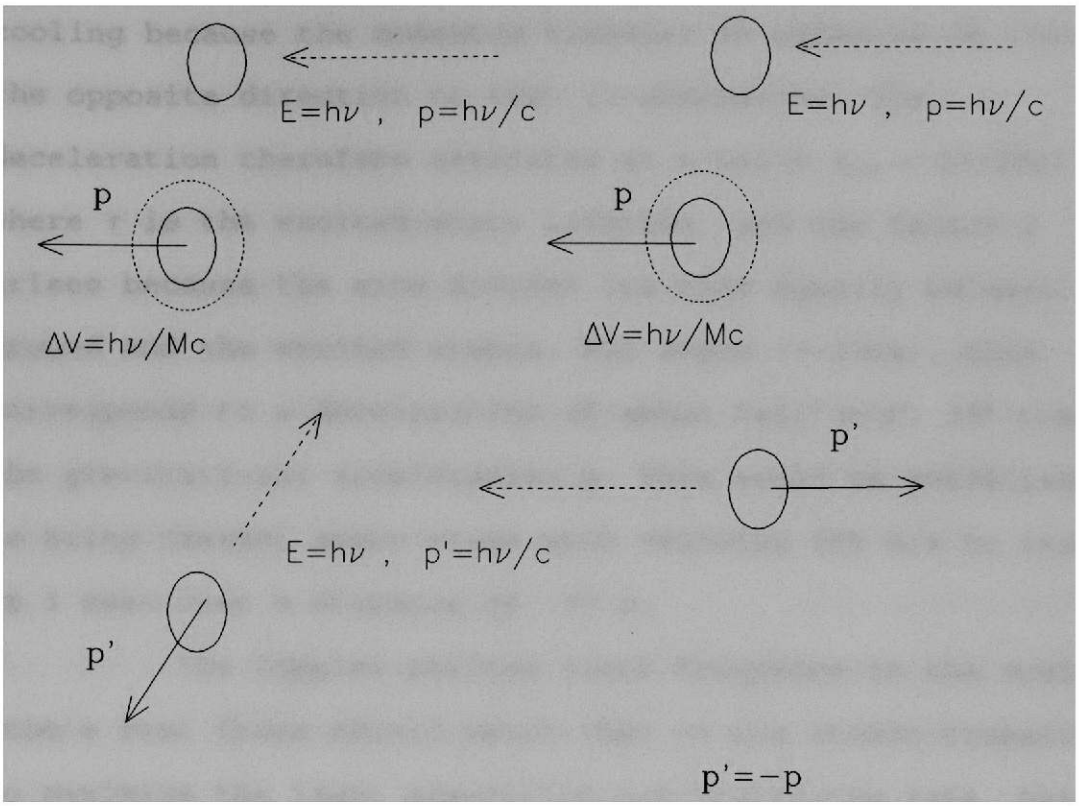

Figure 1 Absorption and Re–emission Mechanisms. Spontaneous emission of the absorbed photon will lead to the net momentum transfer while stimulated emission will not.

High light intensity can produce faster absorption, but it also causes equally fast stimulated emission; the combination produces neither deceleration nor cooling because the momentum transfer in emission is then in the opposite direction to that in absorption. The deceleration therefore saturates at a value $a_{max} = h\nu/2Mc\tau$, where τ is the excited-state lifetime, and the factor 2 arises because the atom divides its time equally between the ground and the excited states. For argon (τ~30ns), this corresponds to a deceleration of about 2×10^5 m/s², 10^4 times the gravitational acceleration g. This would be sufficient to bring thermal argon atoms with velocity 555 m/s to rest in 3 msec over a distance of .77 m.

The Doppler-shifted laser frequency in the moving atom's rest frame should match that of the atomic transition to maximize the light absorption and scattering rate. This rate is given by the Lorentzian:[18]

$$\Gamma_{sc} = \frac{\gamma s/2}{1 + s + (4\pi)^2 \frac{(\delta - \Delta\nu_d)^2}{\gamma^2}} \qquad (1)$$

Where $s = I/I_{sat}$ is the ratio of the light intensity I to the saturation intensity I_{sat}; $\delta = \nu_r - \nu_l$ is the detuning of the laser frequency ν_l from the atomic resonance frequency ν_r; $\Delta\nu_d = \nu_r v/c$ is the Doppler shift corresponding to velocity v and $\gamma = 1/\tau$. For maximum deceleration, $\delta - \Delta\nu_d$ must be chosen

to be nearly zero so that the laser is in resonance with the atom having velocity v in its rest frame. The net force on an atom will be $F=h\nu_r\Gamma_{sc}/c$ and saturates at large **s** to $h\nu_r/2\tau$.

As the atoms in the beam slow down, their changing Doppler shift will take them out of resonance with the (spectrally narrow) laser, and they will eventually cease absorb and decelerate. A velocity change of a few m/s will correspond to a Doppler shift decrease of a few times the natural linewidth of the optical transition (typically few MHz). For example, a velocity change of 8 m/s will correspond to a Doppler shift decrease of 2 times the natural linewidth of the optical transition in Argon (5.3 MHz for a cycling transition used in this experiment). The result is that only a small number of atoms in the beam (those with the correct initial velocity, such that they "see" the laser frequency near in resonance) are slightly decelerated by the few m/s needed to take them out of resonance with the laser. The production of a very narrow hole in the velocity distribution comes about as those atoms that were initially nearly resonant with the laser are pushed to lower velocities where they pile up as they go out of resonance and no longer experience significant changes in their velocities. This type of cooling is called "pushing" or nonresonant cooling. A hole burned in the velocity distribution constitutes the first clear experimental demonstration of laser cooling of an atomic beam.

B. TECHNIQUES OF BEAM DECELERATION

To cool a large fraction of the atoms in an atomic beam by a significant amount, it is necessary to compensate for the change in Doppler shift that takes the atoms out of resonance with the cooling laser. There are two ways to keep the laser in resonance with the decelerating atoms. One is to change the laser frequency as the atoms decelerate ("chirp cooling").[19] By sweeping (or chirping) the laser frequency from ν to $\nu+\Delta\nu$ to keep it resonant with the Doppler-shifted decelerating atoms, all atoms with velocity slower than the initially resonant velocity v_i are swept into a narrow velocity group around v_f ($v_i-v_f=\lambda\Delta\nu$). Since there is a maximum acceleration (a_{max}), there is a maximum frequency scan rate $\nu_{max} = a_{max}/\lambda$. If the frequency scan rate ν is larger than ν_{max}, the atom's Doppler shift cannot change rapidly enough and the atom will go out of resonance. If the scan rate is lower than ν_{max}, and there is sufficient power, the atomic velocity will adjust itself to be just far enough out of resonance, that the scattering rate produces the required rate of change of Doppler shift. This technique is complicated because is very hard to keep the laser frequency tuned while scanning at the necessary rate.

The second approach to the Doppler shift problem is to change the frequency of the atomic transition rather than that of the laser. This can be achieved using a spatially varying magnetic field along the beam path to

Zeeman shift the atomic resonance frequency so as to keep the atoms in resonance with a fixed-frequency cooling laser. This "Zeeman cooling"[20] differs from chirp cooling in that it is a continuous process, whereas chirp cooling produces pulses of cooled atoms at the end of each laser frequency scan. Zeeman cooling has the advantage of producing all of the cooled atoms in the same quantum state. This can be particularly advantageous for trapping or collision experiments. In addition, Zeeman cooling produces a spatial compression of atoms because all atoms are brought to rest (or to some final velocity) at the same location in the magnetic system.

Both Zeeman and chirp cooling can produce large reductions in the atomic velocity as well as compression of the velocity spread. Strictly speaking, only the velocity compression should be called "cooling", but often the term is used to include deceleration as well. For chirp cooling, the compression takes place in time (all affected atoms are instantaneously in resonance with the changing laser frequency); for Zeeman cooling it takes place in space (all affected atoms are resonant at a point in space and therefore at the same velocity).

This experiment was performed using the Zeeman cooling to compensate for the change in Doppler shift that takes the atoms out of resonance during the laser cooling process.

C. ZEEMAN COOLING

When an atom is under the influence of an external magnetic field, the energy levels of an atom are shifted (Zeeman effect), and as long as the shift of the ground and excited states is different, the energy difference between them and hence the resonant frequency of an atomic transition induced by the laser will also be shifted. The shift of the resonant frequency for an atom in magnetic field, $\Delta\nu_z=\Delta E_z/h$, can be calculated, and the field tailored to compensate the appropriate Doppler shift along the moving atom's path.

For atoms having initial velocity v_o and decelerating at a constant rate a, the atomic velocity as a function of a distance z is:

$$v(z)=(v_o^2-2az)^{1/2} \qquad (2)$$

For a linear Zeeman shift to compensate the changing Doppler shift, the appropriate field profile must vary as:[20]

$$B(z)=B_0(1-x)^{1/2} \qquad (3)$$

Where $x=2az/v_o^2$ and the initial magnetic field B_o ($B_o=hv_o/\mu_B\lambda$) is the field which produces a Zeeman shift equal to the Doppler shift of an atom having velocity v_o.

Some atoms in a thermal velocity distribution are moving too fast to be decelerated at all because, for them, the laser frequency is Doppler shifted too far out of resonance to absorb light, even where the magnetic field is strongest at the magnet system entrance. Others have velocities (equal to or less than v_o) whose Doppler shift causes the laser frequency to match the magnetic-field shift and begin slowing down as soon as they enter the system. Still others are moving so slowly that they do not absorb light until they have traveled to a point where the static but spatially varying magnetic field has decreased to the appropiate value to match their smaller Doppler shift and produce resonance. Thus all atoms with velocity lower than v_o can be decelerated to some smaller velocity. This final velocity is determined by the resonance condition at the chosen laser frequency in the field at the end of the magnet system. All cooled atoms are swept into a narrow velocity group around this final velocity. The result is that the originally wide thermal velocity distribution is compressed and shifted to lower velocities.

Other field profiles are allowed, but because of the existence of a maximum possible acceleration there is also an upper limit on the field gradient given by:

$$\frac{d\nu}{dB}\frac{dB}{dz}\cdot v \leq a_{max}/\lambda \qquad (4)$$

Where $d\nu/dB$ depends on the Zeeman effect. This restriction is equivalent to the restriction on the scan rate of the laser in chirp cooling.

Argon has a cycling transition at 811.73 nm (cycles of excitation and decay involve only two states). The lower state is a $1S_5$ J=2 metastable state and acts as a ground state; the upper excited state is a $2P_9$ J=3 state with lifetime $\tau \sim 30ns$[21]. The natural linewidth of the transition $\gamma = 1/2\pi\tau$ is about 5.3 MHz (Figure 2).

In a magnetic field, the energy levels of an atom split according to their projection m_j of the total angular momentum onto the magnetic field direction. The quantization axis is defined along the axis of the atomic and laser beams. The laser light is circularly polarized and carries angular momentum. The direction of polarization is chosen to be σ^+, so that the atoms absorbing the light must increase the projection of their angular momentum ($\Delta m_j = +1$).

For argon atoms in the J=2 m_j=2 sublevel of the $1S_5$ metastable state, the only state to which they can be excited is then J=3 m_j=3 sublevel of the $2P_9$ excited state. The other possible σ^+ transitions are shown in Figure 3. The selection rules for transitions between m_j components of different electronic states ($\Delta m_j = \pm 1, 0$) guarantee that after many cycles of absorption-emission, all the atoms, regardless of their initial m_j, eventually end up in the states with highest projection of angular momentum, cycling

on the J=2 m_j=2 → J=3 m_j=3 transition. Imperfect polarization or misalignment of the laser and magnetic field axes allows unwanted transitions and this will end the cooling process of the atoms.

For transition between $1S_5$ J=2 m_j=2 and $2P_9$ J=3 m_j=3 states in argon, the energy shift produced by a magnetic field of magnitude B (measured in Tesla) will be $\Delta E_z=(3g_{13}-2g_{12})\mu_B B$, where μ_B is the Bohr magneton and g_1 is the Landé g-factor of each state. Assuming[22] g_{12}=1.506 and g_{13}=1.338, $\Delta E_z \approx \mu_B B$ eV and the corresponding frequency shift $\Delta\nu_z \approx 1.4\times10^{10} B$ (measured in Hz) or $\Delta\nu_z \approx 14$ GHz/Tesla=1.4 MHz/G. In this case, the condition given in Eqn. 4 can be evaluated as follow:

$$dB/dz \leq 1760/v \text{ [Gauss/cm]}$$

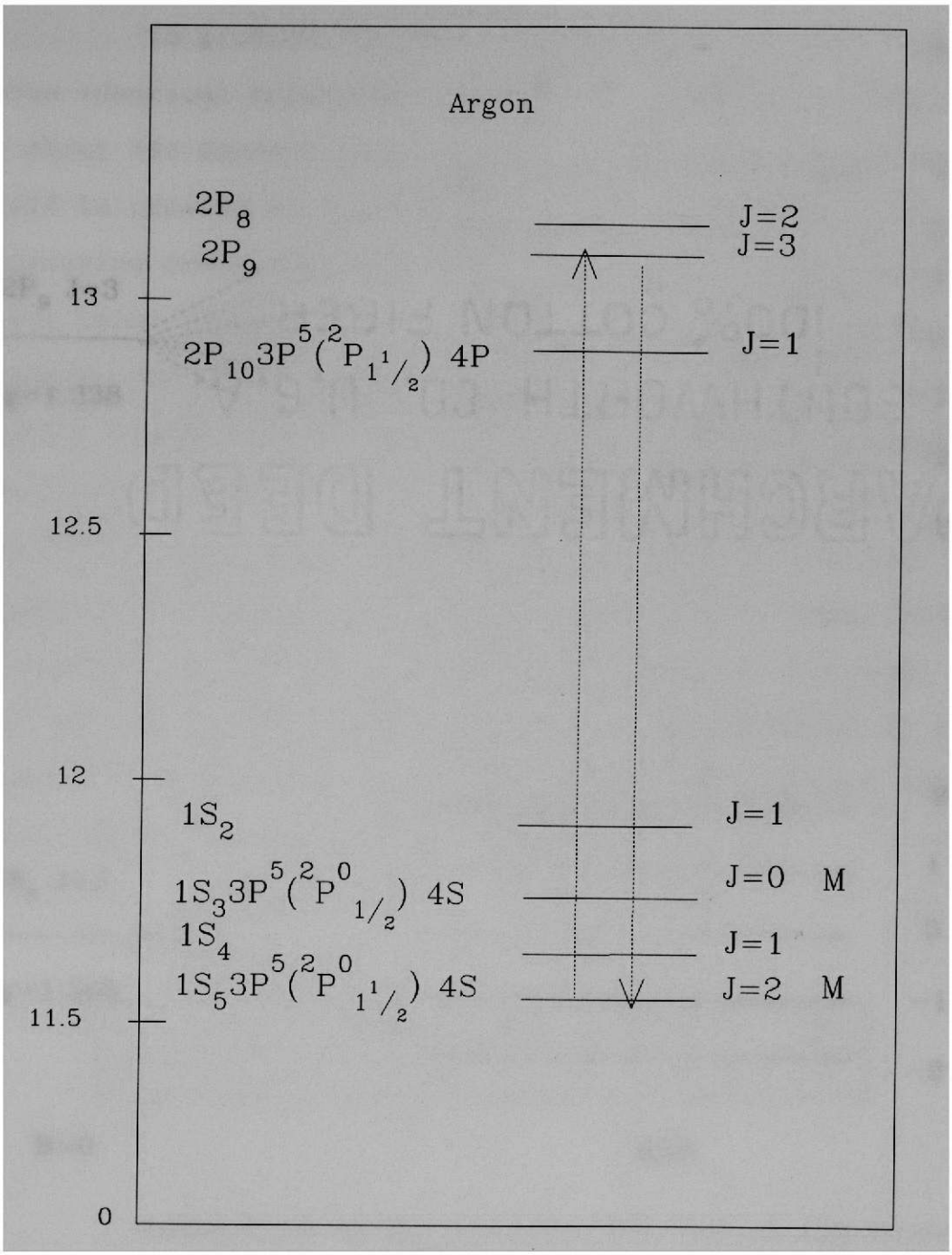

Figure 2 Energy Level Diagram for Argon.
The cycling transition is from the $1S_5$ J=2 metastable state at 11.5477 eV to the $2P_9$ J=3 state at 13.047 eV.

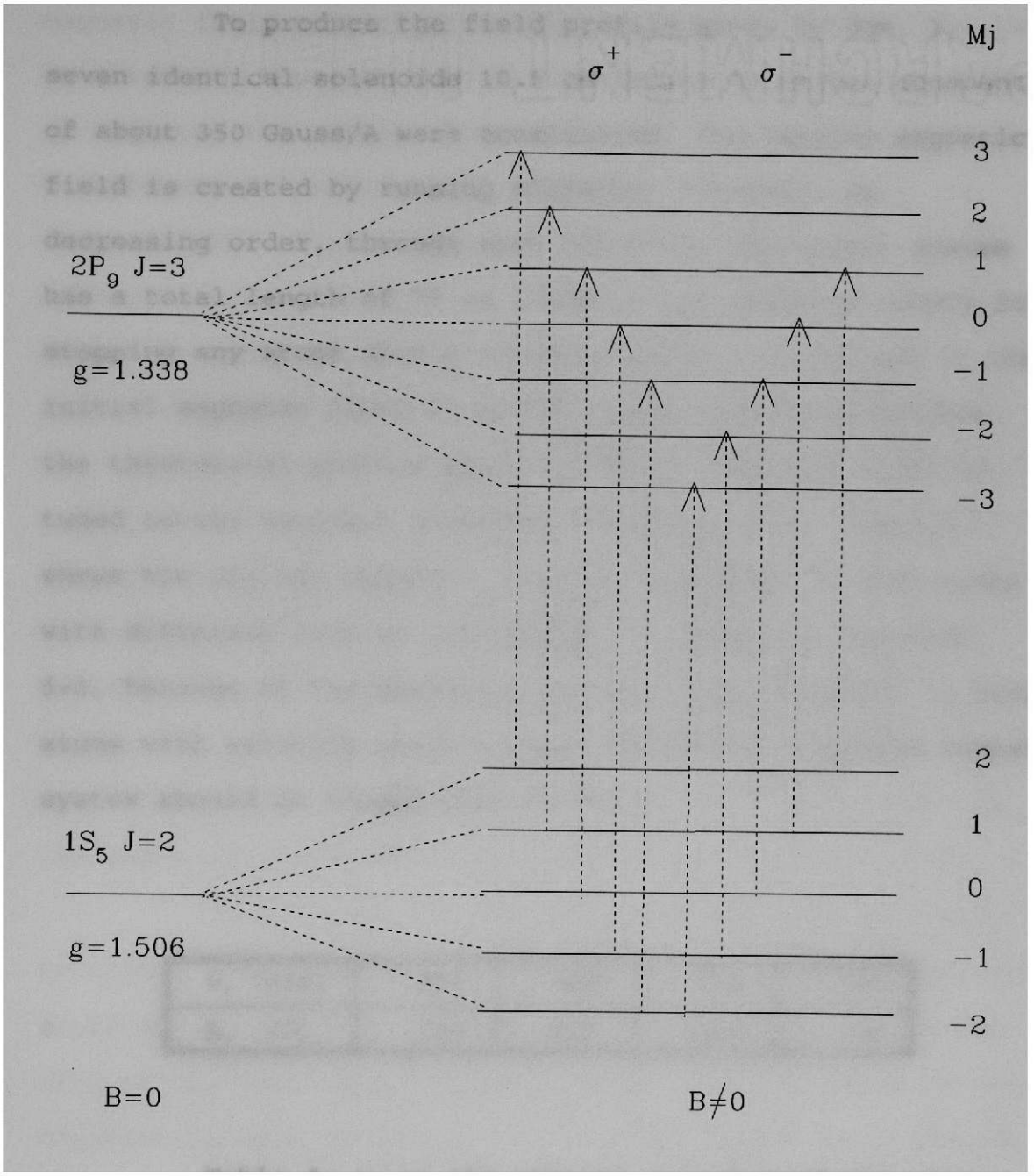

Figure 3

Zeeman splitting of the transition $1S_5$ J=2 − $2P_9$ J=3. The σ^+ ($\Delta M_j = +1$) and σ^- ($\Delta M_j = -1$) transitions are shown.

D. MAGNET SYSTEM

To produce the field profile given by Eqn. 3, seven identical solenoids 10.5 cm long with magnet constants of about 350 Gauss/A were constructed. The tapered magnetic field is created by running different currents, in decreasing order, through each solenoid. The magnet system has a total length of 77 cm. This is the required length for stopping any atoms with a velocity below v_o = 555 m/s if the initial magnetic field B_o is 490 Gauss, the field follows the theoretical profile given by Eqn. 3, and the laser is tuned to the resonant frequency (detuning δ=0). Table I shows the initial magnetic field B_o necessary to stop atoms with different initial velocities, v_o, when the detuning δ=0. Because of the maximum attainable deceleration, to stop atoms with velocity greater than 555 m/s the required magnet system should be longer than 77 cm.

v_o (m/s)	800	600	400	200
B_o (G)	703	527	352	176

Table I. v_o is the initial velocity of the atoms and B_o is the necessary initial magnetic field to stop the atoms with v_o.

By adjusting the current in each magnet, a magnetic field very close to the theoretical requirement can be obtained. However, because of the gap between each pair of magnets, the actual tapered magnetic field does not have a uniformly decreasing gradient. We call this effect the "edge effect". Figure 4 shows the measured magnetic field when the current in all the magnets is constant. The edge effect introduces a relative error of about 6% for a magnetic field produced when the current in all magnets is 1A; the error decreases as the magnetic field is lowered. A comparison between the theoretical and the measured tapered magnetic fields for two different sets of currents is shown in Figure 5 (B_o=490 Gauss). At the first gap, the magnetic field is about 6% different from the expected magnetic field; and the difference gets smaller as the current decreases in the last magnets. This small "edge effect" on the magnetic field should not affect the cooling process.

In the Table II are shown the currents necessary to create a tapered magnetic field with an initial magnetic field 490 Gauss. The currents were taken comparing the two sets of currents used in Fig. 5, such that the ratio of the currents in each magnet, I/I_1, is close to the ratio $B(z)/B_o$ in the center of the corresponding magnet (I_1 is the current on the first magnet and B(z) is the magnetic profile given by Eqn. 3).

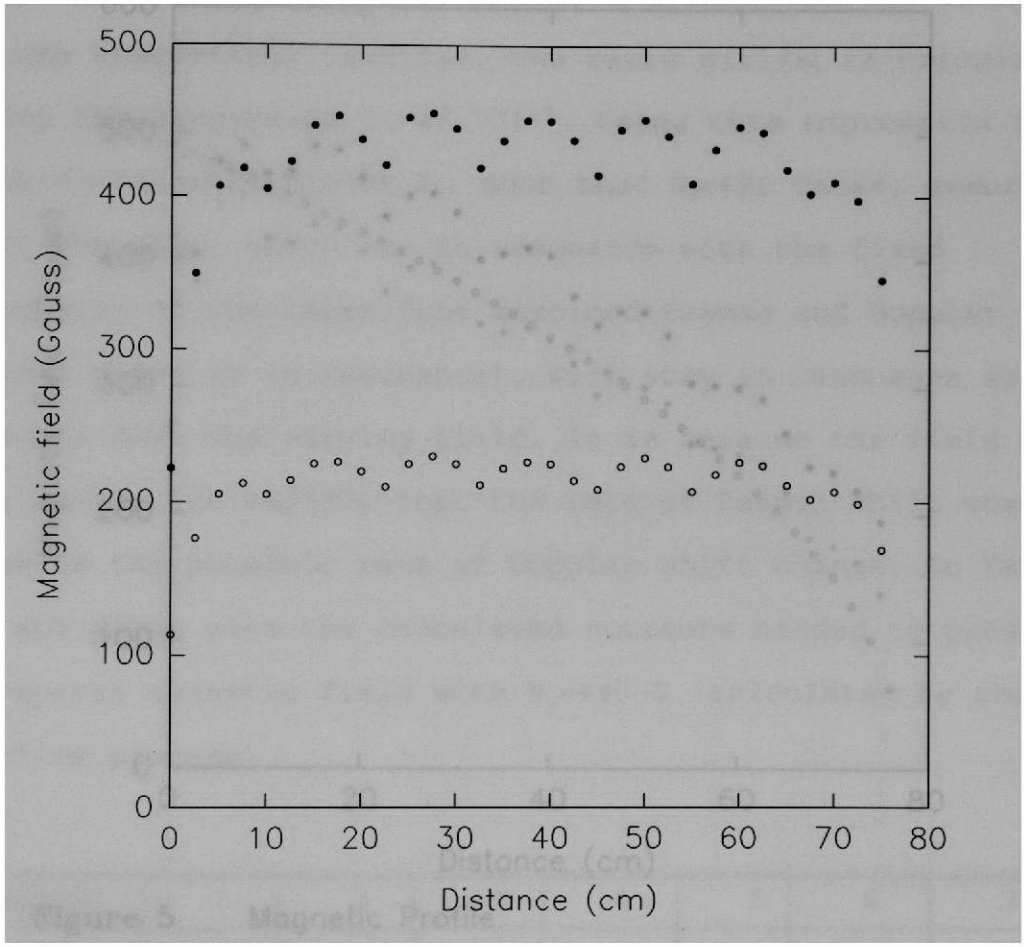

Figure 4 MEASURED CONSTANT MAGNETIC FIELD.

Hollow circles— I=.5A in all the magnets
Filled circles— constant current in all the magnets I=1A.

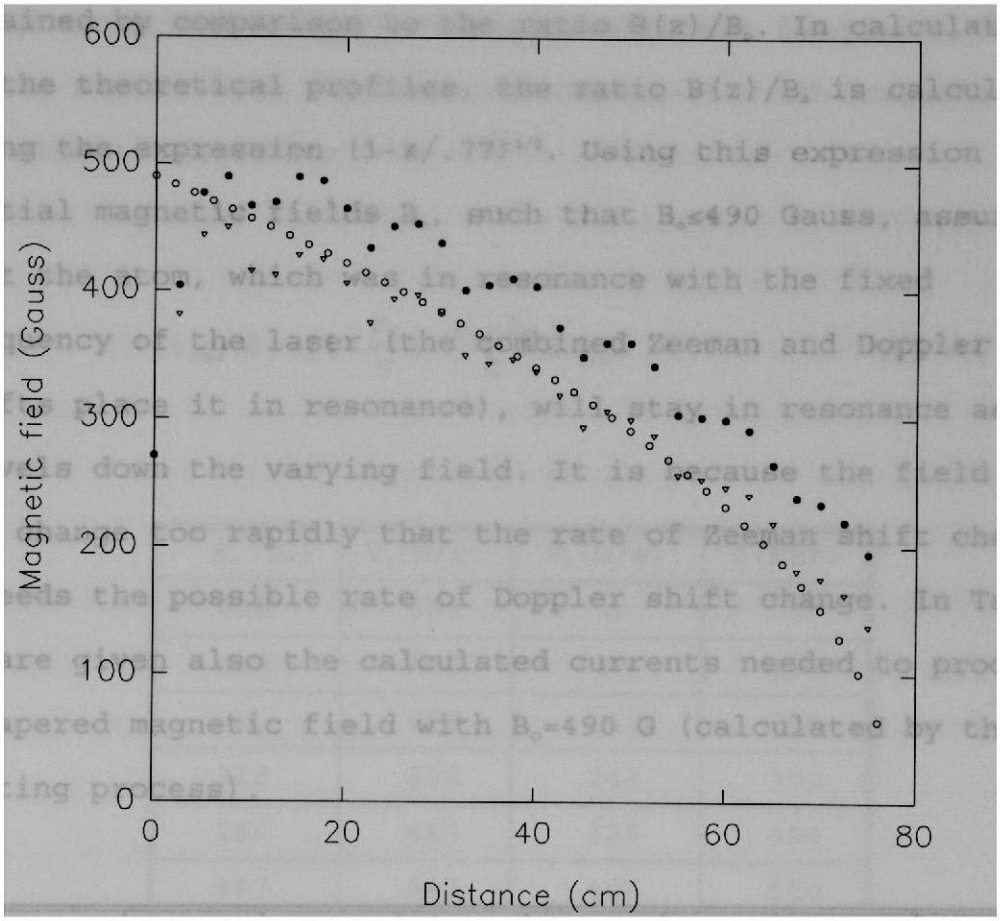

Figure 5 Magnetic Profile.

Hollow circles– Theoretical profile calculated by Eqn. 3 for an initial magnetic field 490 Gauss.
Filled circles– Measured tapered magnetic field (TMF) with the currents: 1.2, 1.1, 1.0, .91, .81, .67, .54
Hollow triangles– Measured TMF profile with the currents : 1.2, 1.03, .92, .79, .7, .55, .35.
All the currents measured in A.

Actually, for different initial magnetic fields, the currents needed to produce the magnetic profile given by Eqn.3 are obtained by fitting the calculated magnetic field to the theoretical profile by the least squares method. The currents obtained by this method are very close to those obtained by comparison to the ratio $B(z)/B_o$. In calculation of the theoretical profiles, the ratio $B(z)/B_o$ is calculated using the expression $(1-z/.77)^{1/2}$. Using this expression for initial magnetic fields B_o, such that $B_o \leq 490$ Gauss, assures that the atom, which was in resonance with the fixed frequency of the laser (the combined Zeeman and Doppler shifts place it in resonance), will stay in resonance as it travels down the varying field. It is because the field does not change too rapidly that the rate of Zeeman shift change exceeds the possible rate of Doppler shift change. In Table II are given also the calculated currents needed to produce a tapered magnetic field with B_o=490 G (calculated by the fitting process).

Magnet	1	2	3	4	5	6	7
I_{meas} (A)	1.21	1.05	.9	.75	.69	.53	.3
I_{calc} (A)	1.22	.9	.87	.74	.65	.52	.43

Table II. I_{meas} - Set of currents obtained by comparison the two sets of current used in Fig.3. I_{calc} is the set of currents obtained by the fitting process.

If the laser is tuned below the frequency of the resonant absorption ($\delta \neq 0$), deceleration can be achieved to a certain final velocity ($v_f = \delta\lambda$). In this case the initial magnetic field B_o and the corresponding initial velocity v_o should vary as shown in Table III. V_o was calculated from Eqn.2 and B_o matching the "Doppler-shifted" frequency, seen by the atoms, with the resonant Zeeman-shifted frequency of the atomic transition:

$$(\nu_{res} - \delta) \cdot (1 + \frac{v_0}{c}) = \frac{\mu_B \cdot B_0}{h} + \nu_{res} \cdot \qquad (5)$$

B_o (G)	V_o(m/s)	V_f(m/s)	δ(MHz)
490	555	0	0
422	560	81	100
365	578	162	200
318	606	243	300
280	643	325	400
247	687	406	500
220	738	487	600

Table III. δ is the laser detuning; v_f is the final velocity corresponding to the detuning δ, v_o is the initial velocity that may have the atoms to decelerate to v_f if the initial magnetic field is B_o.

Chapter III - RADIATION SOURCE

Lasers are particularly desirable to cool atoms because of their intrinsic characteristics. Laser light is highly monochromatic, unidirectional, intense and a wide range of optical frequencies is accessible. A cycling transition for the atom is necessary so that cycles of excitation and decay involve only two states. The excited atom will primarily decay back to the state from which the transition originated thereby leaving the atom ready for another absorption. A transition in argon at 811.73 nm is in the near infrared and accessible with lasers.

The optical system required for cooling incorporates three main components. First is the light source (in terms of type of laser and output frequency). Second includes systems for evaluating the characteristics of the output light (i.e. power, linewidth) and the spectrometers for monitoring the frequency. Finally, the optics that are used to direct the beam into the spectrometers and to introduce the laser beam into the molecular beam apparatus (MBA).

A. LASER SYSTEMS

Two types of laser systems have been used. Initially, in the experiment, a diode laser was used. Using a diode laser, the possibility of burning a hole in the velocity distribution of the metastable atoms emerging from the source (Hole-burning) was demonstrated . These measurements helped to check the alignment of the laser and the atom beam. In order to affect the atoms all along the path, the diode laser was replaced by a titanium:sapphire ring laser capable of greater power output.

A laser diode system[23] used to produce a laser beam at the desired frequency consists of a commercially available laser diode, a collimating lens, and a diffraction grating. The grating serves as part of an external Littrow cavity.[24] The diode's back facet has a high reflectivity coating while the output facet has an anti-reflectivity coating. These two facets form the diode's internal resonance cavity. The laser diode by itself will have multiple output wavelengths (broad linewidth) because several longitudinal modes can operate simultaneously. The diode's output beam is collimated by a lens and is incident on the dispersive diffraction grating. The first-order diffracted light returns into the diode laser forming an external resonance cavity while the zero order diffracted light is the output beam. Rotation of the grating about its vertical axis changes the output frequency. Since the

external and internal cavities will compete with each other for laser gain, the resonant frequency of these two cavities must be matched for efficient operation of the laser system. In effect, the system is forced to operate in a single longitudinal mode. The characteristics of the laser light from the diode at 811.73 nm were: power at the entrance of the beam apparatus less than 15mW/cm^2 and laser linewidth about 50 MHz. The laser linewidth was measured using a Fabry-Perot interferometer and calculated from hole-burning experiments.[25]

The ring laser system (Coherent 899-21) operates as a solid state ring laser using a titanium:sapphire crystal as the gain medium.[26] It is tunable from 680 to 1025 nm. A high power pump laser, a 20W argon Ion laser (Coherent Innova 200), is used as the pump source. The system incorporates passive and active frequency control in order to obtain stable operation in a single longitudinal cavity mode.

All components and stages are mounted directly or indirectly to a 2-inch bar that provides mechanical strength and thermal stability. Unidirectional lasing is achieved with an optical diode. For passive frequency control a series of intracavity frequency filters are used. Active frequency control is achieved with and electronic servo loop and reference cavity. With 15W in the pump beam, we obtain an output power of about 700 mW, and at the entrance of the

atomic beam apparatus approximately 400mW. Using a high resolution Fabry-Perot interferometer the linewidth was measured to be about 5 MHz. The existing frequency drift (approximately 75 MHz/h) limits the narrow linewidth that should be obtained using the active frequency control. Calculations of the laser linewidth from the hole-burning experiments, show $\Delta\nu \approx 15$ MHz.

B. ABSORPTION SPECTROMETERS

Absorption experiments provide a simple way to determine the frequency characteristics of the laser. In the case of argon, a metastable state is the lower state of the cycling transition. The atoms in the metastable state are created in a gas discharge tube (GDT). Because of collisional processes, the atoms may move toward or away from the light source and the absorption line will be Doppler broadened.

To achieve the absorption and saturated absorption measurements, two "probe" laser beams A and B are directed through the discharge tube onto two photodiodes (respectively D_A and D_B). Probe beam A is used for the absorption measurement. The signal from photodiode D_A is converted to a voltage by an I/V amplifier and displayed on a voltmeter. The voltmeter signal is highest when the light is not in resonance with an atomic transition (no absorption occurs) and lowest when the light frequency is in resonance

with the frequency of the transition.

When the laser is tuned to a resonant frequency, ν_{res}, the absorption will be maximum (only atoms with zero velocity relative to the light source in the discharge tube will absorb radiation). If there are two counterpropagating laser beams (from the same source), and one of them produces saturation after passing through the tube, then no more radiation is absorbed from the second one since the same set of atoms absorb the light. This causes a reduced absorption and a Lamb dip in the absorption curve centered on ν_{res}; in this case the absorption of the second beam is minimum.

For the saturated absorption another laser beam is required. This "pump" beam (directed through the discharge tube opposite to the probe beam) will saturate the transition. The output from D_B goes to a lock-in amplifier. The reference signal for the lock-in amplifier is provided by a chopper which chops the pump beam. The lock-in amplifier's output is also monitored by a voltmeter. This voltmeter signal will be maximum when the light is resonant with the transition and minimum when it is not. In this experiment the Lamb dip in the absorption curve is not observed due to the noise in the discharge tube and also because the linewidth of the laser is wider than the linewidth of the atomic transition.

When there is a maximum saturated absorption and a minimum absorption signals the laser is tuned to the

resonant frequency of the cycling transition in argon.

C. OPTICS FOR LASER BEAM DIRECTION

The main beam from the laser system is split with a microscope slide. The strong beam continues through a slow (1 Hz) chopper and a 1/4-wave plate before being directed into the molecular beam apparatus (MBA). The slow chopper allows acquisition of laser on and laser off data at .5 sec intervals to eliminate effects due to instability of the atomic beam source. The 1/4-wave plate converts the linearly polarized light from the laser system into circularly polarized light (σ^+).

The weak beam from the microscope slide is also split by another microscope slide. The weaker of these two, serves as input to a Fabry-Perot interferometer (FPS). The stronger is directed onto a thick beamsplitter. The reflections off the front and back facets of the beamsplitter are used as the probe beams in the absorption spectrometers. The beam that continues through the beamsplitter is reflected back into the gas discharge tube; this will be the pump beam for saturated absorption measurements.

All the mirrors used in directing the laser beam into the molecular beam apparatus are gold-coated to minimize power loss. Standard aluminum mirrors are used to reflect the pump beam in the saturated absorption

spectrometer, since power loss is not a major concern in this case.

A diagram showing the spectrometers and the optics used in the experiments is shown in Figure 6.

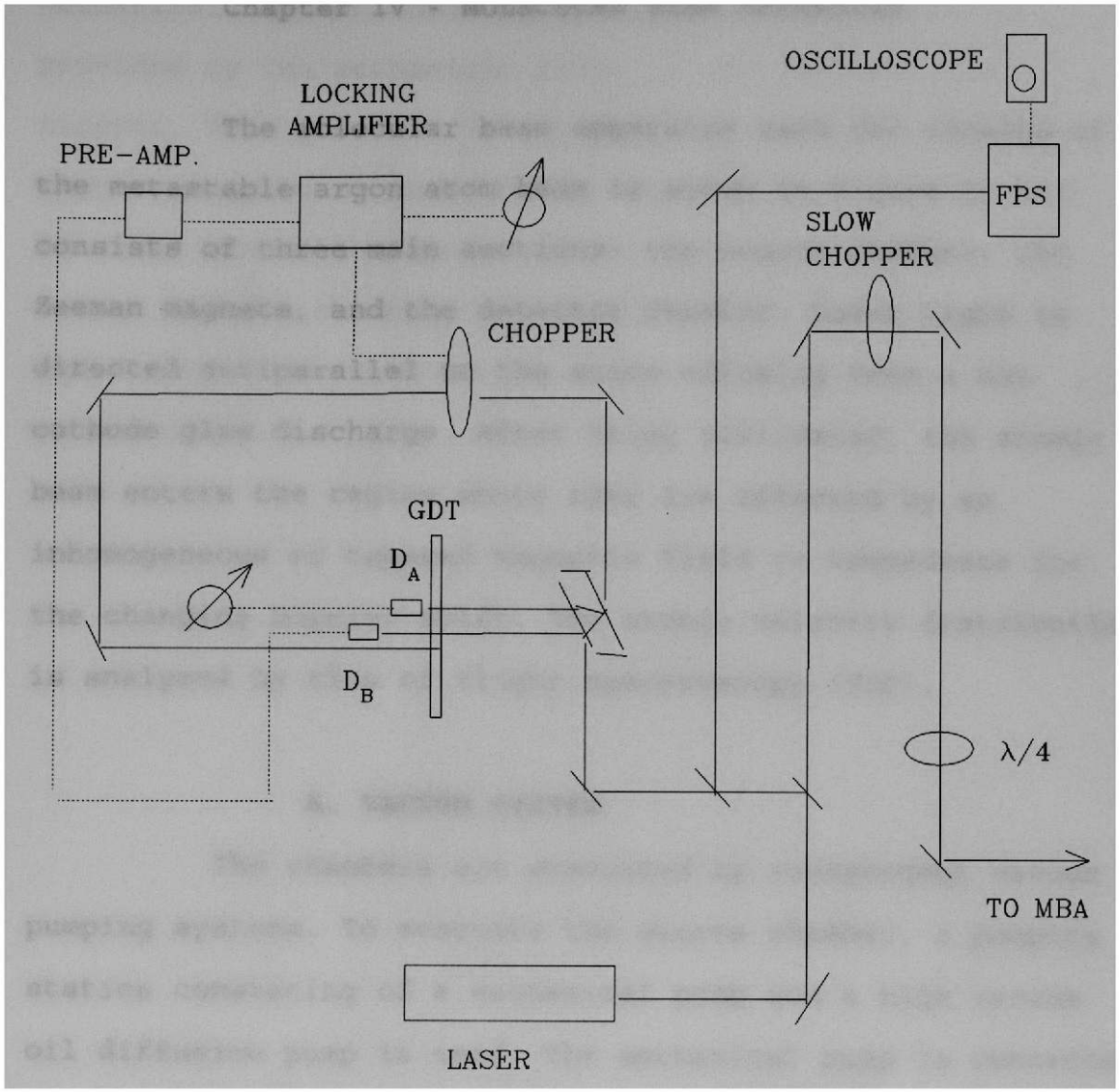

Figure 6 Schematic of Optical Components of the Experiment.

Chapter IV - MOLECULAR BEAM APPARATUS

The molecular beam apparatus used for cooling of the metastable argon atom beam is shown in Figure 7; it consists of three main sections: the source chamber, the Zeeman magnets, and the detector chamber. Laser light is directed antiparallel to the atoms effusing from a hot cathode glow discharge. After being collimated, the atomic beam enters the region where they are affected by an inhomogeneous or tapered magnetic field to compensate for the changing Doppler shift. The atomic velocity distribution is analyzed by time of flight spectroscopy (TOF).

A. VACUUM SYSTEM

The chambers are evacuated by independent vacuum pumping systems. To evacuate the source chamber, a pumping station consisting of a mechanical pump and a high vacuum oil diffusion pump is used. The mechanical pump is connected separately to the source chamber (roughing line), and to the foreline of the oil diffusion pump. It provides a roughing pressure of approximately 10 microns and, with the diffusion pump operating, provides a foreline pressure of 15 microns. In order to know the foreline and roughing pressures, thermocouple gauges are used. In the roughing and foreline sections of the source chamber, PVC lines are used.
The pumping system in the detector chamber consists of two

mechanical and two turbo-molecular pumps. The pressure provided by the mechanical pumps is approximately 10 microns. This pressure is monitored by two thermocouple gauges, mounted on each of the turbo- molecular pumps. Hot filament ionization gauges are used to measure the high vacuum in both chambers. The pressure in the chambers is maintained at about 7×10^{-7} torr. All high vacuum pumps are water-cooled.

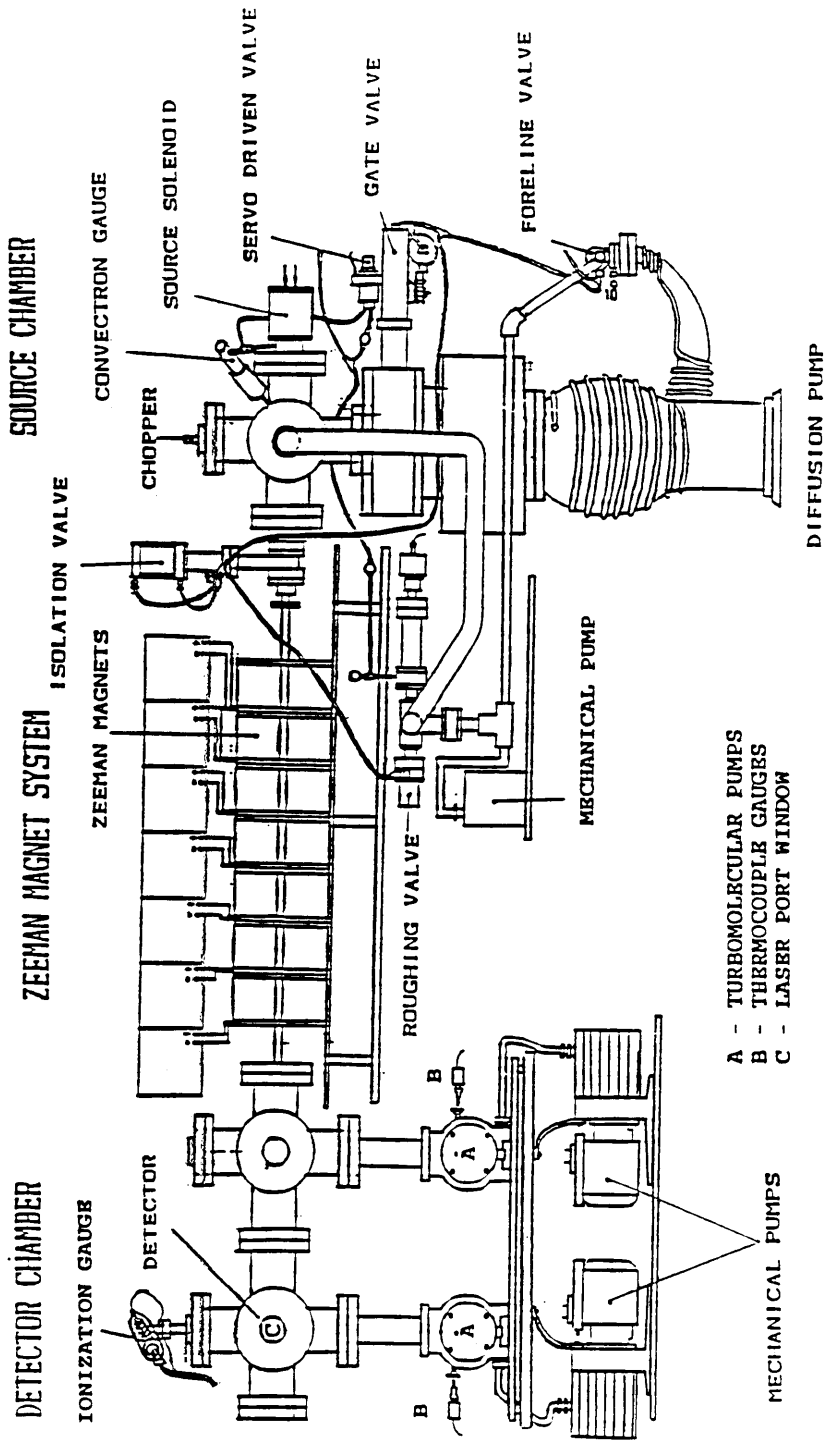

Figure 7 Molecular Beam Apparatus. The flight path length is 1.824 m.

B. SOURCE

The source of the metastable atom beam is a Penning ionization discharge. The 1000 W, 500 V high voltage power supply maintains about 50 V between the cathode (filament) and anode (the flange with an exit slit) during typical operating conditions and supplies the approximately 400 V necessary to initiate the discharge. The thoria-coated tungsten filament produces electrons which are accelerated towards the anode by the potential difference across the discharge. The electrons collide with the gas forming a mixture of photons, metastable atoms, ions, neutral and Rydberg atoms that effuse through a circular exit (.71 mm diameter) in an aluminum anode at the end of 3 cm long Pyrex tube, where the discharge occurs. The filament current varies between 10-15 A, and is used to control the discharge current, which typically is about 300 mA.

The gas supplied to the discharge enters the tube through a servo-driven valve which is part of an automatic pressure controller. The pressure in the discharge tube is monitored by a convectron gauge and maintained at about 7 mTorr.

Intensity is especially important for a metastable state noble gas beam, since only a fraction of the total neutral beam is in the desired state. It has been demonstrated,[27] that a longitudinal magnetic field, applied to a low pressure, hot cathode glow discharge, will increase

the intensity of metastable atoms effusing from a central anode slit. To provide this magnetic field, a solenoid is mounted on the discharge tube such that the axial magnetic field constrains the discharge along the axis between the filament and the exit slit to a smaller radius. A high current on a source magnet will also increase the number of ions effusing from the source. This is an undesirable effect since the background will increase considerably when the magnet system is turned on. For this reason, in place of the current that will maximize the yield of metastable atoms, a current of .6 A, corresponding to a magnetic field of about 70 Gauss, is used on the source magnet.

Once the discharge products effuse from the slit, they are continuously chopped by an aluminum wheel of 7.91 cm in diameter. The chopper has 2 diametrically opposed 0.081 cm slits and is driven by a synchronous motor at a frequency of 60 Hz. The chopper slit and rotational speed give an open time of approximately 100 μsec and a beam pulse rate of 120 Hz, which allows sufficient time (8.3 msec) to observe nearly the complete thermal time-of-flight (TOF) distribution in each pulse. After passing through the chopper, the beam is collimated with a .008 cm slit.

When the chopper is open, the light from a light-emitting diode (LED) stimulates a photo-transistor. The LED and the photo-transistor are located at opposite sides of the chopper wheel, such that, the stimulation of

the photo-transistor can be achieved only when the chopper is open. The signal generated by the transistor is amplified and delayed in order to assure coincidence with photoelectron pulses from the ultraviolet (UV) photons which come down the beam path when the chopper opens. This signal is used as a reference or start signal for the TOF spectroscopy. A pair of sweep plates, operating at 300 V/cm normal to the beam, electrostatically remove charged particles and ionize atoms in long-lived Rydberg states from the beam, leaving only metastable and neutral atoms in the ground state within the beam.

C. DETECTOR AND TIME OF FLIGHT ANALYSIS

At the end of the flight path, photons and atoms are detected by measuring electrons ejected from a gold mirror by either the photoelectric effect or Auger effect. These electrons are collected and amplified by an electron multiplier (Channeltron detector). The detector and the gold mirror are mounted on an aluminum plate, that is supported by two fixed rods and is connected to a linear motion feedthrough. The gold mirror is negative biased relative to the entrance cone of the electron multiplier; consequently, the ejected electrons are attracted into the electron multiplier. This entrance cone is biased at -2000 volts and the exit of the detector is operated at -200 volts. The gold mirror is used as a source of electrons as well as a

reflecting mirror for the laser. The laser enters the detector chamber through a vacuum port window and is directed antiparallel to the atom beam after reflecting from the gold mirror. As a result, the beam is irradiated by the laser along the entire flight path (1.824 m): from the source exit slit to the gold mirror in the detector chamber.

The beam path length guarantees sufficient TOF for all excited atoms to undergo optical decay before reaching the detector (except for the metastable atoms). On the other hand, only metastable atoms and photons have sufficient energy to eject electrons from a gold mirror. The ground-state atoms in the beam (unless they are product of the dissociative recombination in the source)[28] have kinetic energy less than the work function of the gold (5.1 ev), and therefore are not detected.

D. DATA ACQUISITION

The signal from the electron multiplier is pulse-shaped and amplified. A constant timing single channel analyzer reduces the background noise, and gives the input pulses to the ORTEC ACE Multichannel scaler (a hardware and software package that performs data collection and MCS emulation) operating in a Zenith personal computer.

The detection system measures the arrival time of the metastable atoms and photons. The TOF spectra of the

metastable atoms are recorded in channels 40 μsec wide and the sweep length is 200 channels (the time/channel constant is 40 μsec). Since the path length is known, the velocity distribution of the metastable atoms can be obtained as a function of their TOF. The velocity resolution of the TOF method is only limited by the chopper open time. For Δt_c=100 μsec, $\Delta v = v(1+.4 \times \text{Channel})^{-1}$. For velocity 200m/s, the resolution is Δv=2.5m/s. As the atom's velocity decreases, the resolution of the method is better. A typical TOF distribution is shown in Figure 8. Metastable atoms in the beam that effuse from a Maxwellian velocity distribution in the discharge have a TOF distribution $f(t)$ normalized to N total counts given by:[29]

$$f(t) = \frac{C}{t^5} \exp\left[-\frac{5}{2}\left(\frac{t_p}{t}\right)^2\right] \qquad (6)$$

Where $t_p = mL^2/5kT$ is the most probable TOF and $C = (25N/2)t_p^4$. In addition to the TOF distribution of Maxwellian origin there is a faster distribution of atoms (not shown in the Fig. 8), some of which may be in the ground state. These fast atoms are products of dissociative recombination reactions in the discharge and are discussed elsewhere.[30,31] The data fall below the equation 6 curve in some region $t > t_p$ due to small-angle elastic scattering along the path by the slower atoms.

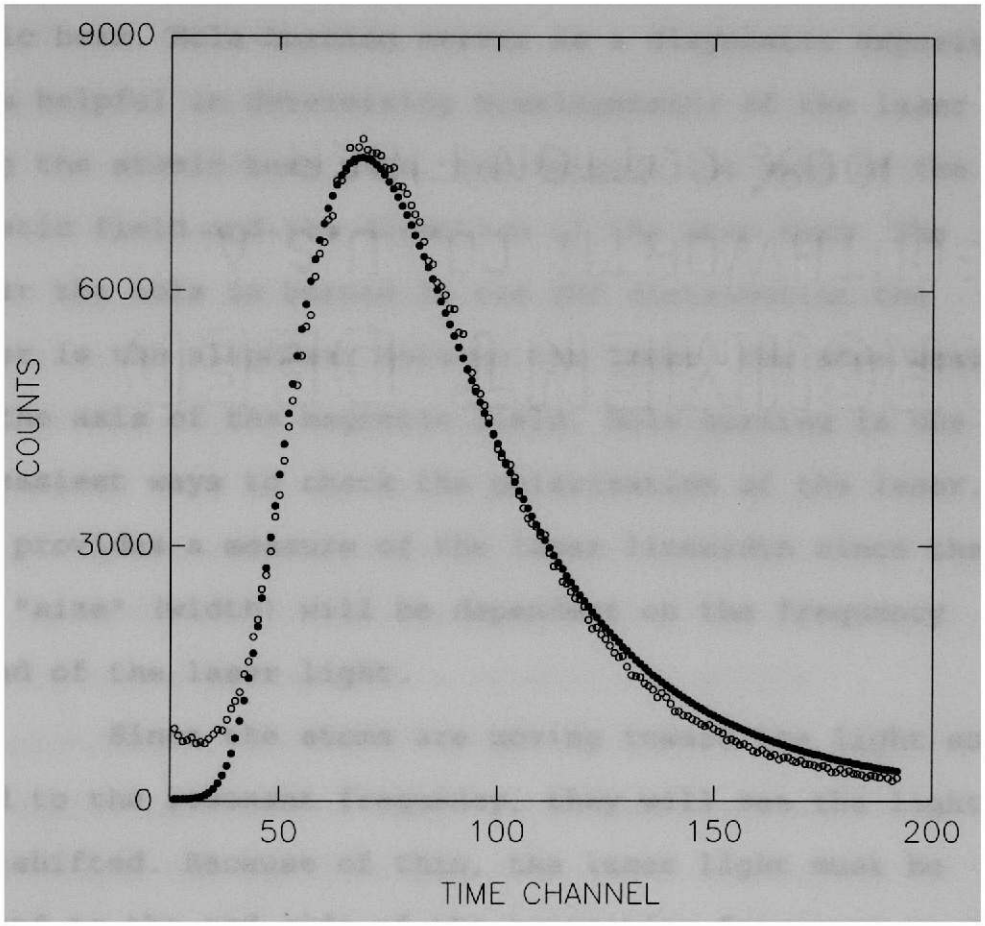

Figure 8 Typical TOF Distribution of metastable Argon atoms (Hollow circles). The time/channel is 40 μsec. Filled circles – Distribution fitted to Eqn. 6.

CHAPTER V - ATOMIC COOLING EXPERIMENTS

A. HOLE-BURNING EXPERIMENTS

The hole burned in the TOF (or, equivalently, in the velocity) distribution, both by laser detuning and by Zeeman shifting of atomic transitions, constitutes the first clear experimental demonstration of laser cooling of an atomic beam. Hole-burning serves as a diagnostic experiment. It is helpful in determining misalignments of the laser along the atomic beam path, and between the axis of the magnetic field and the direction of the atom beam. The deeper the hole is burned in the TOF distribution the better is the alignment between the laser, the atom beam, and the axis of the magnetic field. Hole-burning is one of the easiest ways to check the polarization of the laser. It also provides a measure of the laser linewidth since the hole "size" (width) will be dependent on the frequency spread of the laser light.

Since the atoms are moving toward the light source tuned to the resonant frequency, they will see the light blue-shifted. Because of this, the laser light must be detuned to the red side of the transition frequency so that the frequency of the laser will be in resonance for the atoms moving with some velocity v and, thus, burn a hole in the distribution at the channel corresponding to that velocity (Channel x 40 μsec = 1.824/v). If the detuning δ is

taken to compensate the Doppler shift corresponding to a velocity v ($\delta=\nu_r v/c$), there will be a dip in the velocity distribution at the initial velocity for these atoms and a corresponding bump at the velocity to which they were decelerated. The laser linewidth will cause some broadening around this velocity. This is known as hole-burning. If the detuning is changed to another frequency (but still on the red side of the transition frequency), there will be a shift in the velocity at which the hole-burning occurs.

Hole-burning measurements were taken for several laser detunings. The intensity of the laser light was, at least, 25 times greater than the saturation intensity of the cycling transition in Argon (approximately 4mW/cm^2). Dips in the time distribution corresponding to the slowed atoms were observed as well as the corresponding bump at the later time when the atoms were detected. A detuning of 600 MHz(red) from the resonance frequency compensates for the Doppler shift of atoms moving with a velocity of 487m/s, corresponding to a time of flight of 4.27ms or channel 93. The results for various laser detunings are summarized in Table IV and the TOF distributions shown in Figures 9-12.

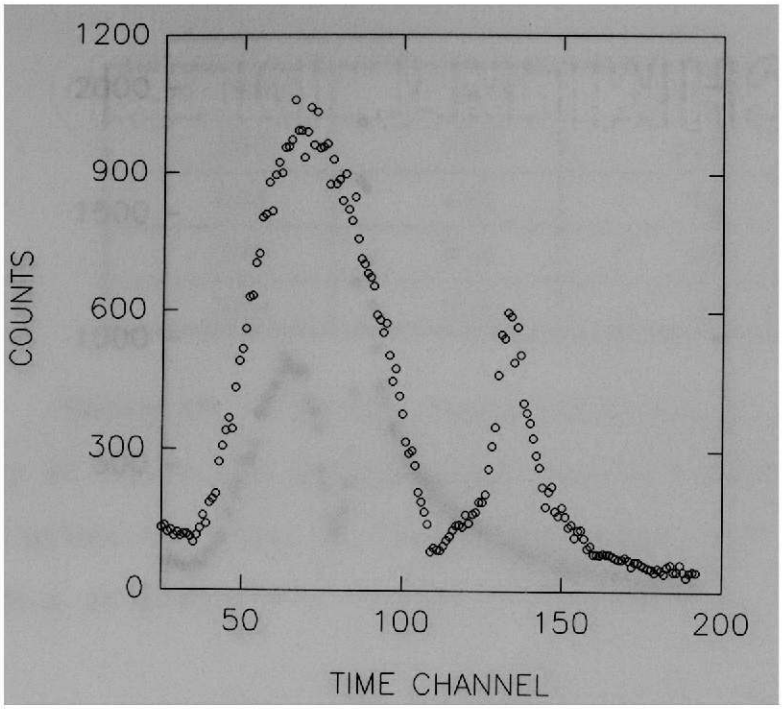

Figure 9 TOF Distribution with the laser detuned 500 MHz Red from resonance.

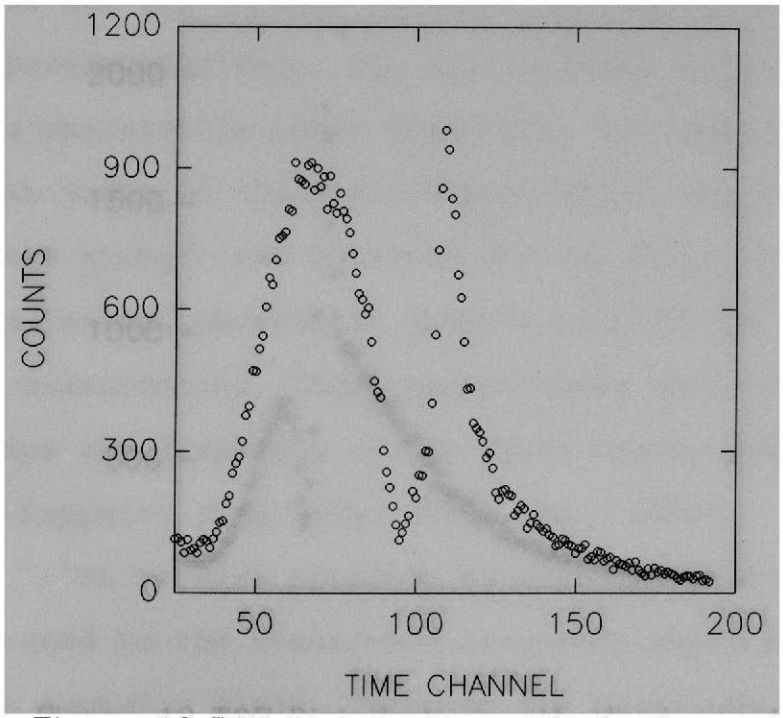

Figure 10 TOF Distribution with the laser detuned 600 MHz Red from resonance

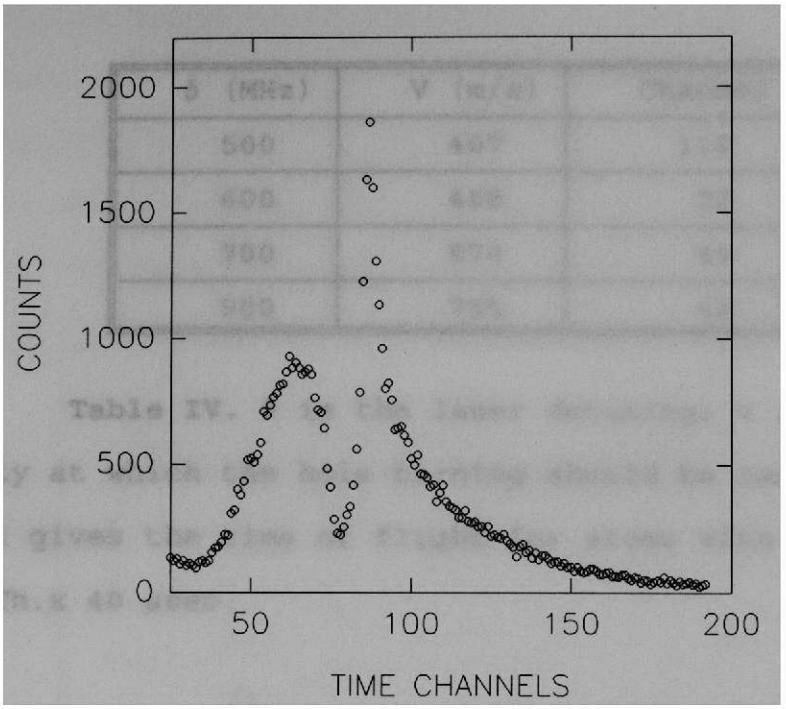

Figure 11 TOF Distribution with the laser detuned 700 MHz Red from resonance.

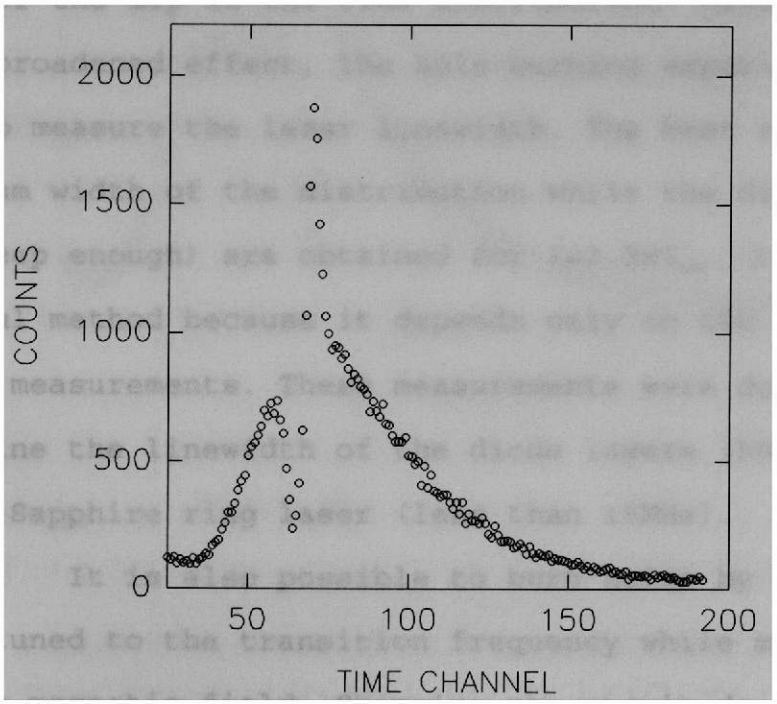

Figure 12 TOF Distribution with the laser detuned 900 MHz Red from resonance

δ (MHz)	V (m/s)	Channel
500	407	112
600	488	93
700	570	80
900	735	62

Table IV. δ is the laser detuning; v is the velocity at which the hole-burning should be centered; the channel gives the time of flight for atoms with velocity v TOF = Ch.x 40 μsec.

Figure 13 shows the power-broadened effect on the width of the dip in the time distribution. Minimizing the power-broadened effect, the hole-burning experiments can be used to measure the laser linewidth. The best results (minimum width of the distribution while the dip is still seen deep enough) are obtained for $I \approx 2.5 \times I_{sat}$. It is a powerful method because it depends only on the time of flight measurements. These measurements were done to determine the linewidth of the diode lasers (50MHz) and of the Ti-Sapphire ring laser (less than 15MHz).

It is also possible to burn holes by keeping the laser tuned to the transition frequency while maintaining a uniform magnetic field. Changing the magnitude of the magnetic field will shift the velocity at which the hole-burning occurs. A constant magnetic field of 500 Gauss, when

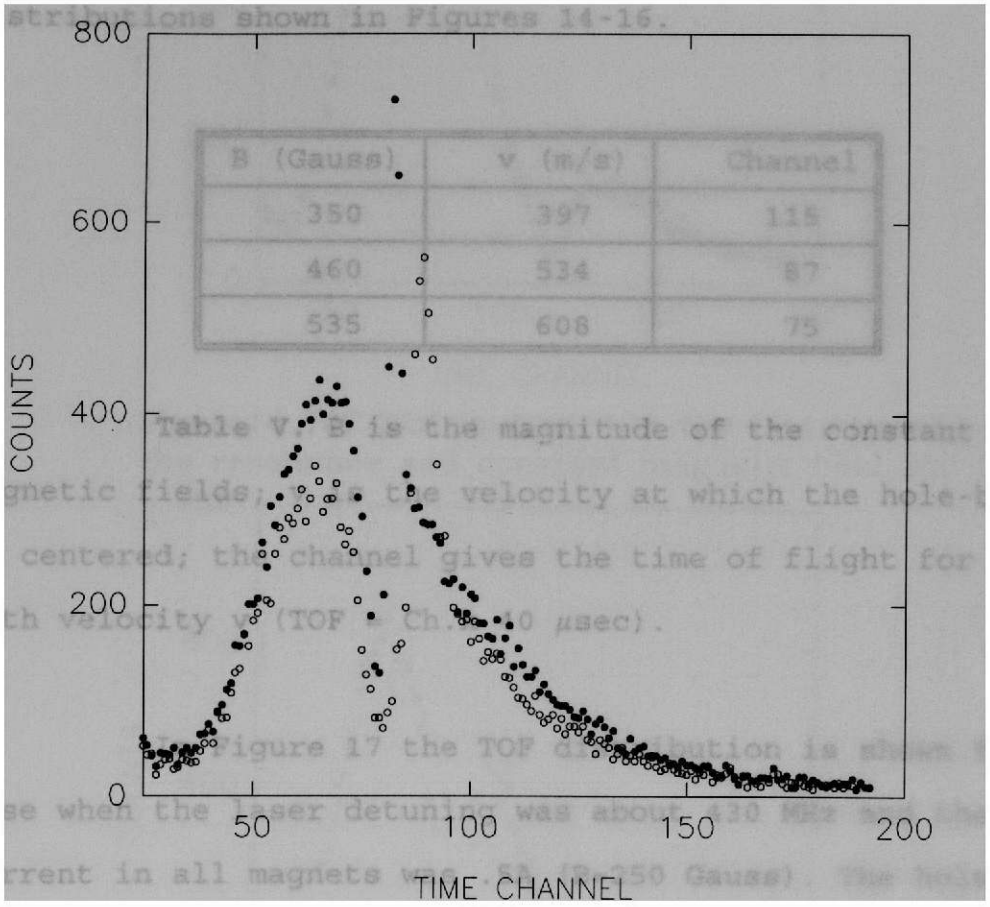

Figure 13

Power broadened effect on the width of the hole burned in the TOF Distribution.
Hollow circles– 100 mW at the entrance of the MBA
Filled circles – 10 mW.

the laser is tuned to the resonance frequency, would compensate for the Doppler shift of atoms moving with a velocity of about 570m/s, corresponding to a time of flight of 3.2ms or channel 80. The results for various constant magnetic fields are summarized in Table V and the TOF distributions shown in Figures 14-16.

B (Gauss)	v (m/s)	Channel
350	397	115
460	534	87
535	608	75

Table V. B is the magnitude of the constant magnetic fields; v is the velocity at which the hole-burning is centered; the channel gives the time of flight for atoms with velocity v (TOF = Ch.x 40 μsec).

In Figure 17 the TOF distribution is shown for the case when the laser detuning was about 430 MHz and the current in all magnets was .5A (B=250 Gauss). The hole from the laser is observed in the channel 131 (velocity 348m/s) and the hole from the magnetic field is in the channel 72 (velocity 632m/s). The hole burned in the distribution due to the magnetic field should be in the channel corresponding to the velocity $v=v_{mag}+v_{las}$, where v_{mag}=284m/s and v_{las}=348m/s (See Eqn. 5).

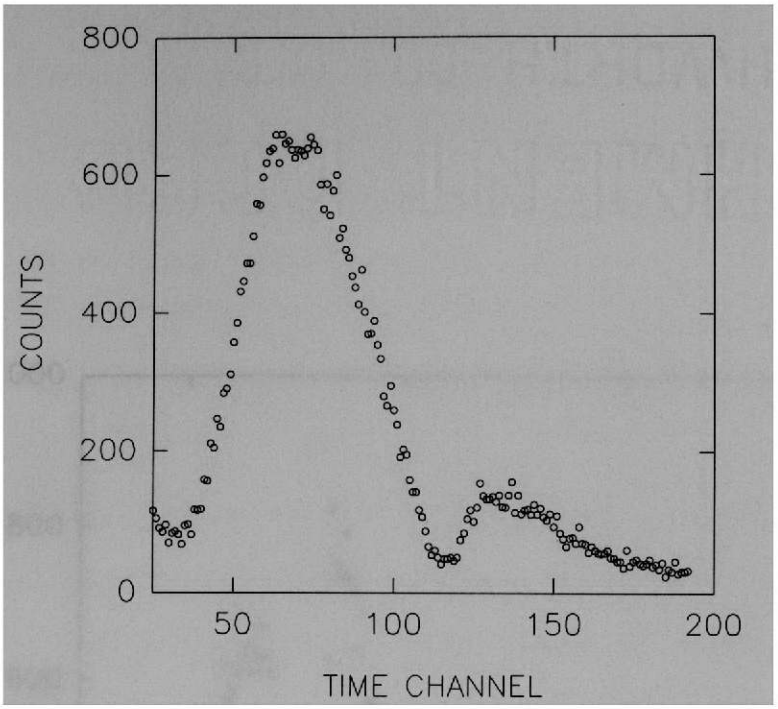

Figure14 TOF Distribution with the laser tuned to the resonance and constant magnetic field 350 G

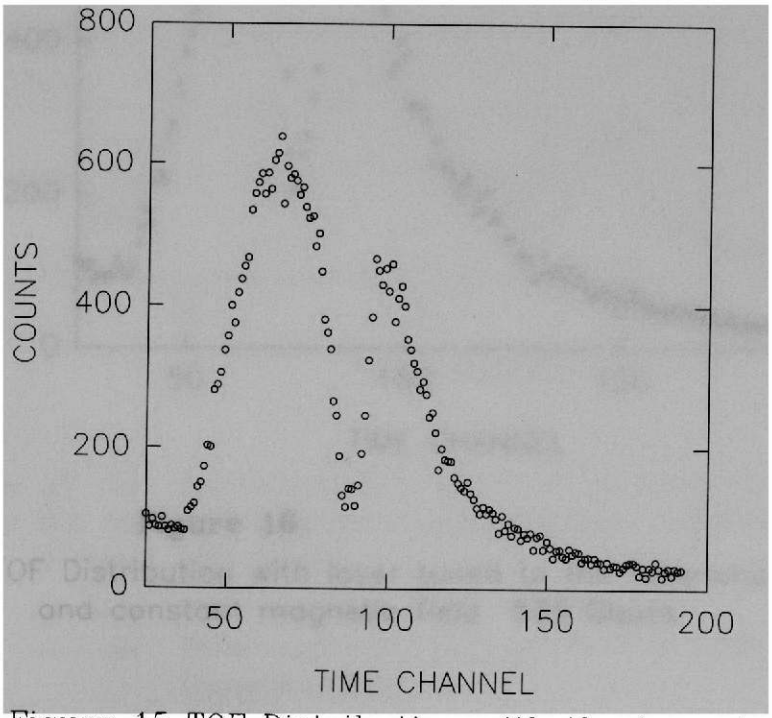

Figure 15 TOF Distribution with the laser tuned to the resonance and constant magnetic field 460 G

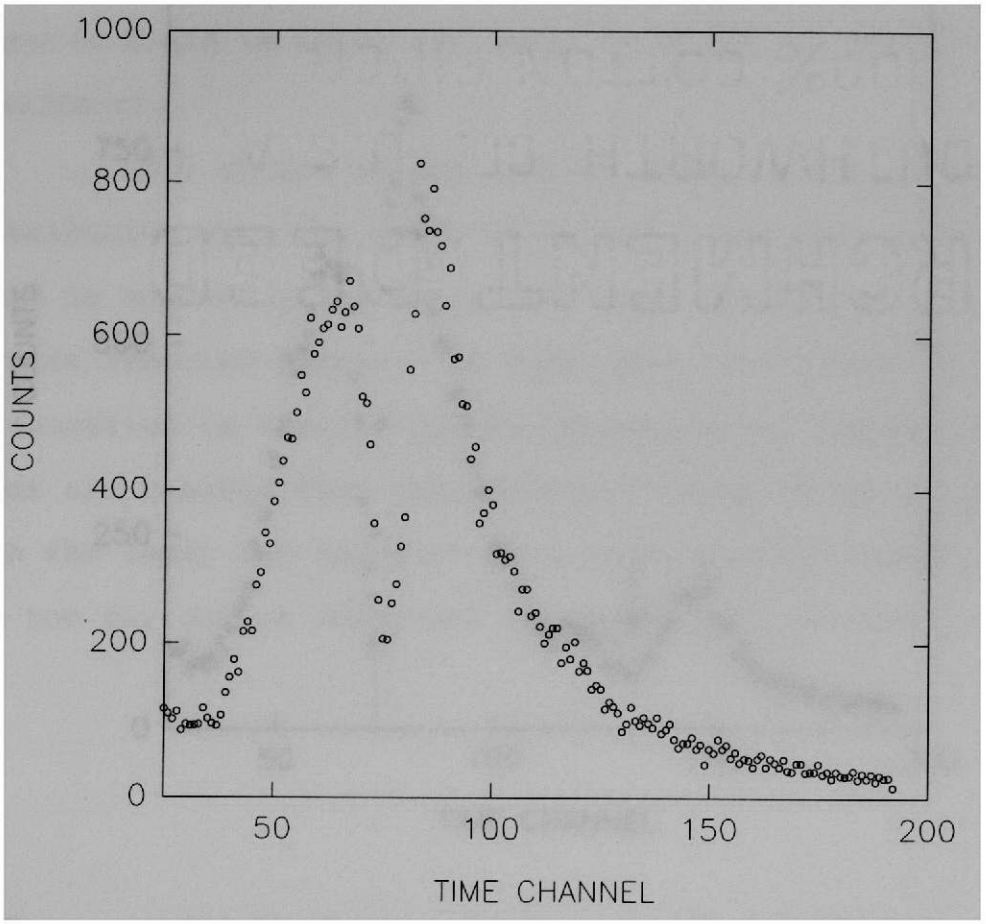

Figure 16

TOF Distribution with laser tuned to the resonance and constant magnetic field 535 Gauss

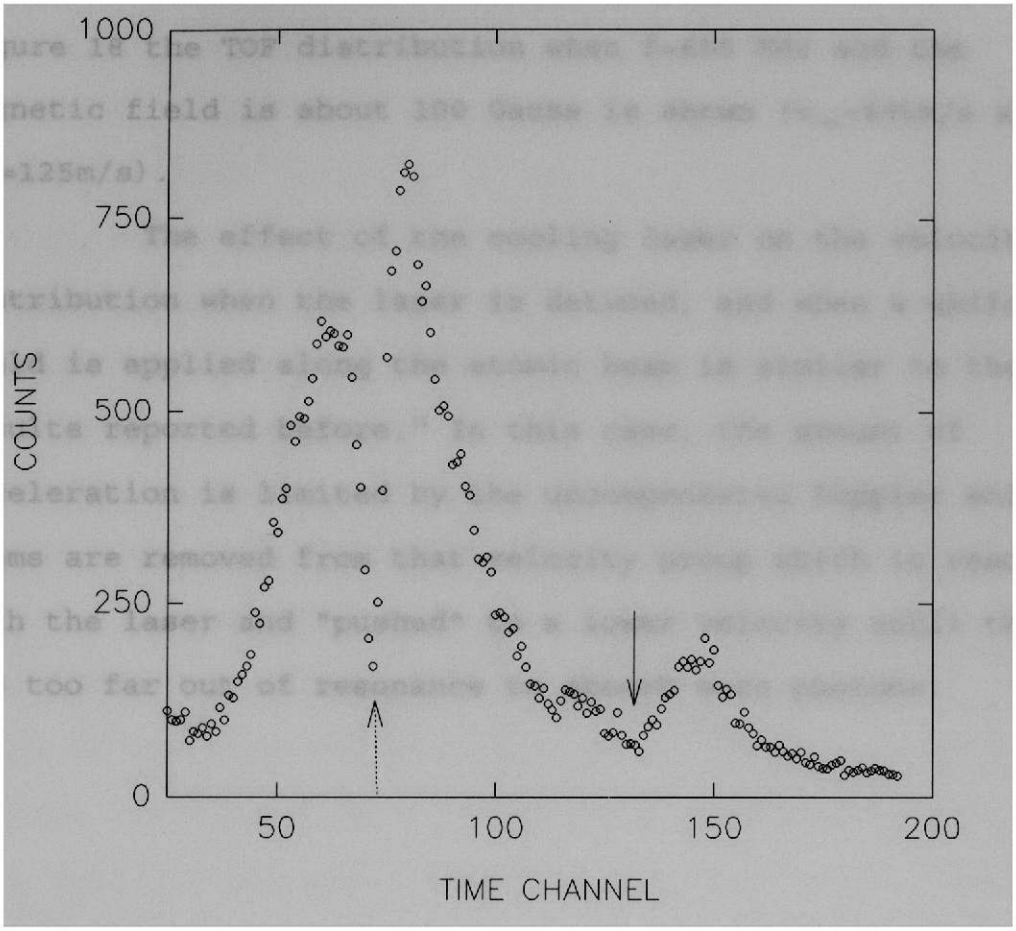

Figure 17 TOF Distribution with the laser detuned 430 MHz from the resonant frequency and constant magnetic field of about 250 Gauss.

——→ Hole-burning from the laser

·····→ Hole-burning produced by a constant magnetic field.

When the laser light is linearly polarized or is not completely circularly polarized, both σ^+ ($\Delta m_j=+1$) and σ^- ($\Delta m_j=-1$) transitions can occurs. For a given detuning of the laser, two symmetrically opposite holes relative to the laser hole-burning, should appear ($v=v_{las}\pm v_{mag}$). In the Figure 18 the TOF distribution when δ=600 MHz and the magnetic field is about 100 Gauss is shown (v_{las}=485m/s and v_{mag}=125m/s).

The effect of the cooling laser on the velocity distribution when the laser is detuned, and when a uniform field is applied along the atomic beam is similar to the results reported before.[32] In this case, the amount of deceleration is limited by the uncompensated Doppler shift. Atoms are removed from that velocity group which is resonant with the laser and "pushed" to a lower velocity until they are too far out of resonance to absorb more photons.

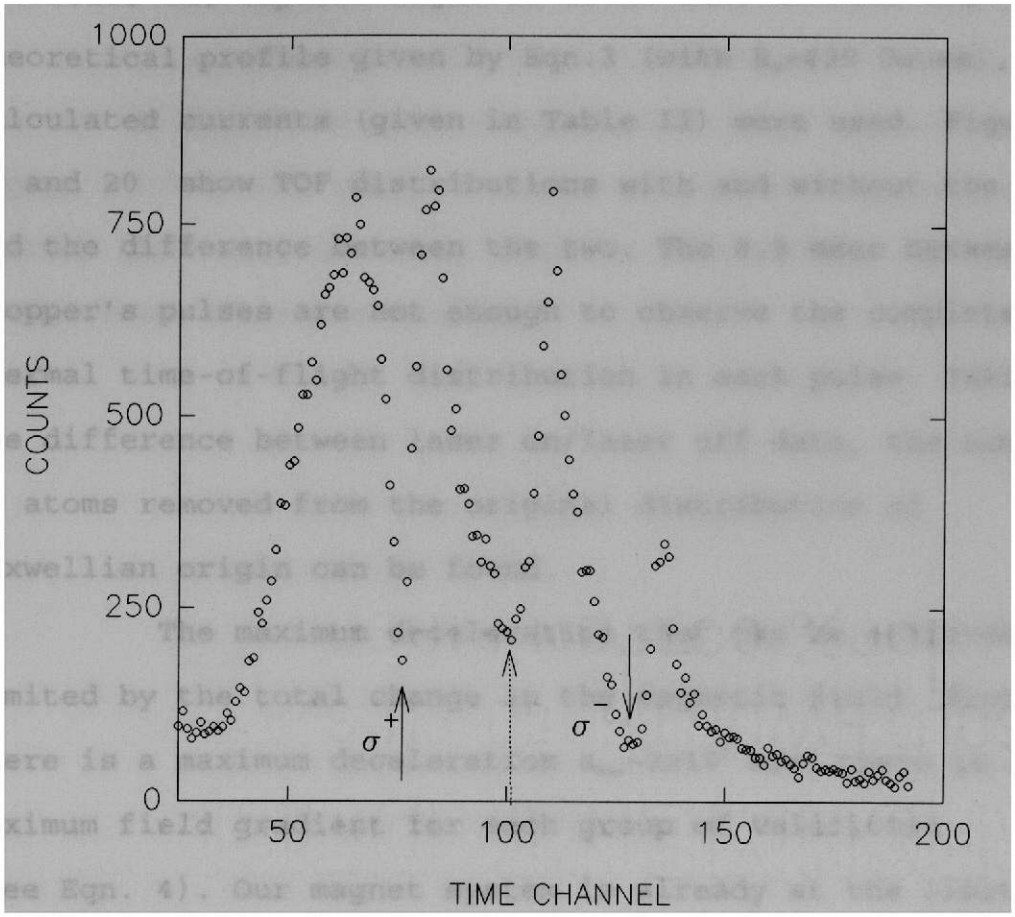

Figure 18 TOF Distribution with the laser detuned 600 MHz from the resonance, constant magnetic field of about 100 Gauss, and laser light linear polarized. The two solid lines show the position of the holes corresponding to a different group of transitions.
--- > Position of the hole burned by the laser.

B. LASER COOLING

Because of the total length of the magnet system (.77 m) and the maximum attainable deceleration, only atoms with a velocity below v_o=555m/s will be stopped or cooled. To create the tapered magnetic field that follows the theoretical profile given by Eqn.3 (with B_o=490 Gauss), the calculated currents (given in Table II) were used. Figures 19 and 20 show TOF distributions with and without the laser and the difference between the two. The 8.3 msec between the chopper's pulses are not enough to observe the complete thermal time-of-flight distribution in each pulse. Taking the difference between laser on/laser off data, the number of atoms removed from the original distribution of Maxwellian origin can be found.

The maximum deceleration that can be achieved is limited by the total change in the magnetic field. Since there is a maximum deceleration $a_{max}=2x10^5$ m/s^2 there is a maximum field gradient for each group of velocities (See Eqn. 4). Our magnet system is already at the limit for atoms with velocity about 500m/s. For this reason, and also because the initial field gradient at the beginning of the varying magnetic field does not follow the theoretical requirement (See Fig.5), the deceleration of the atoms with v_o=550m/s could not be completed from one end of the magnet system to the other.

To achieve greater cooling and to do the cooling process more efficiently (to use more atoms from the atomic beam), a larger change in the magnetic field over a longer path will be needed. Zeeman cooling produces a reduction in the atomic velocity, but to observe the velocity compression the detection scheme should be changed. Instead of measuring the TOF of the atoms when chopper is located before the magnet system, the chopper should be placed after the magnet system. This will give the velocity distribution of the atomic beam after the cooling.

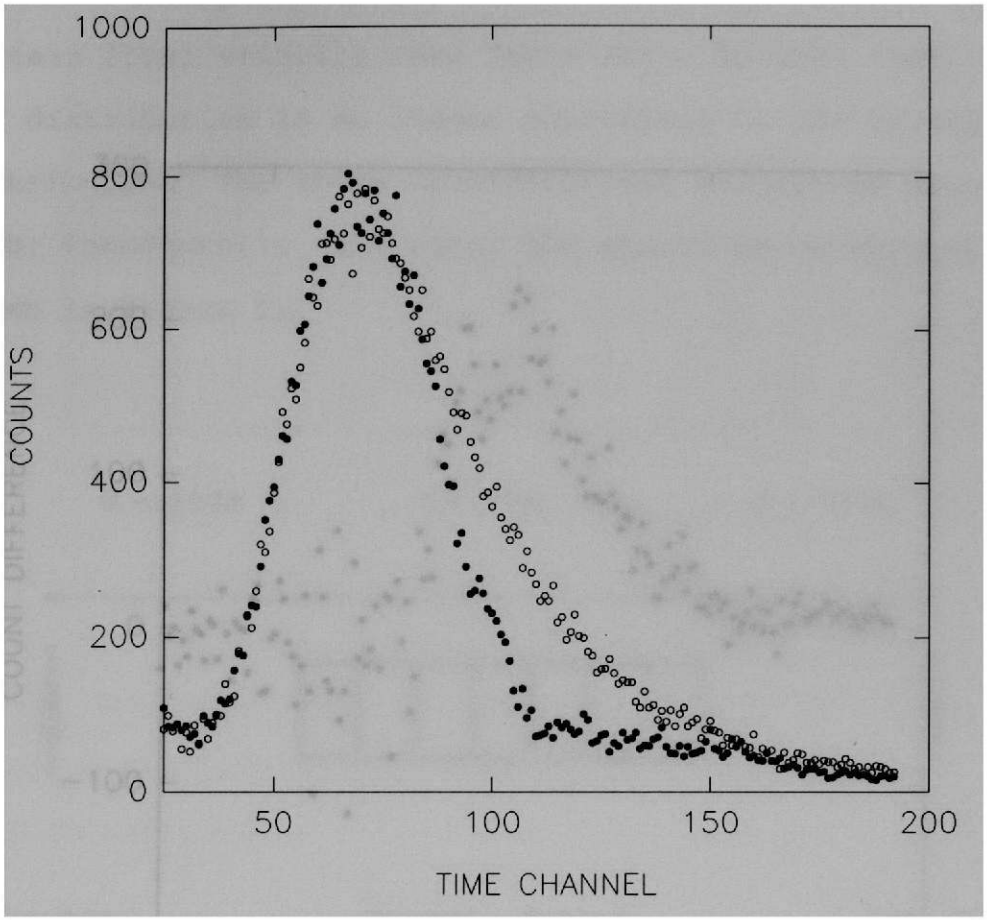

Figure 19 Hollow circles—TOF Distribution of metastable atoms without the laser.

Filed circles—TOF Distribution when the laser is tuned to resonance, and the currents in the magnets to create a tapered magnetic field are given in Table II. B_0=430 Gauss.

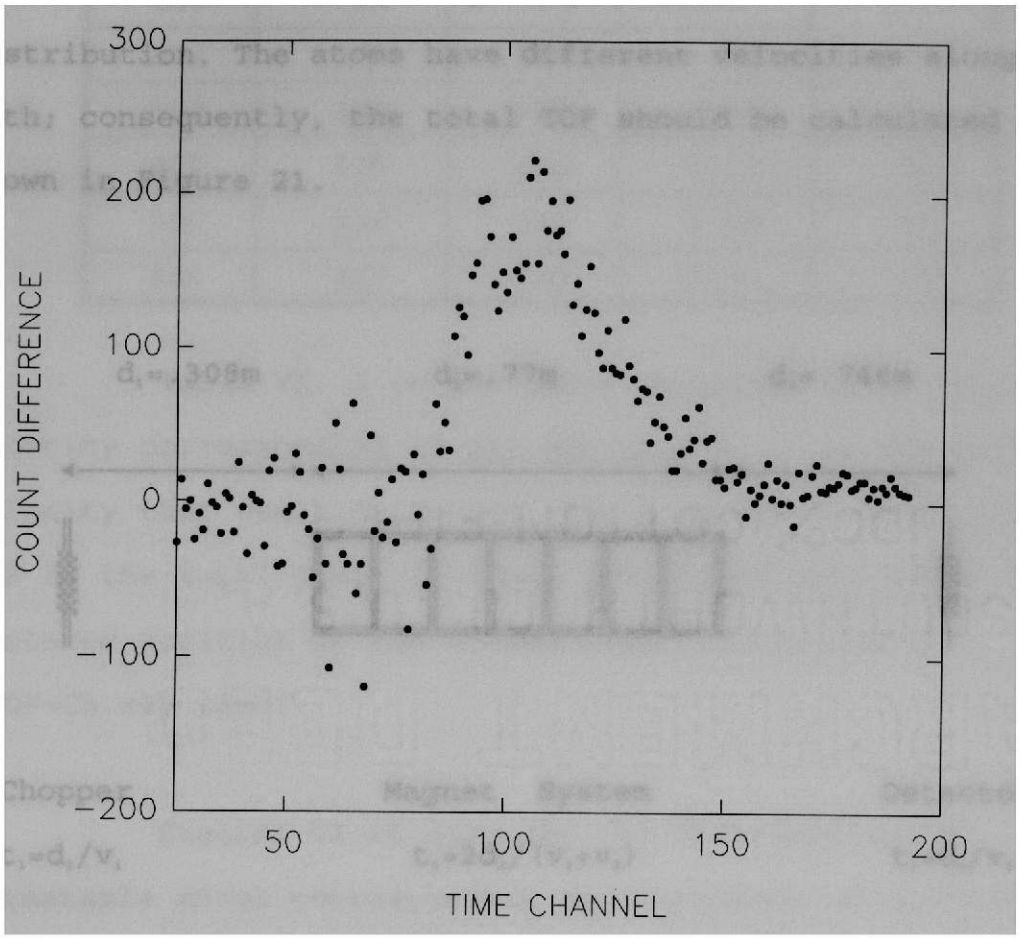

Figure 20

Difference between the two Distributions shown in Figure 19.

To circumvent this problem and really understand the cooling process, the TOF-scheme given before can be used. If the laser is tuned below the frequency of the resonant absorption ($\delta \neq 0$), deceleration can be achieved to a certain final velocity (See Table III). In this case, the TOF distribution is no longer equivalent to the velocity distribution. The atoms have different velocities along the path; consequently, the total TOF should be calculated as shown in Figure 21.

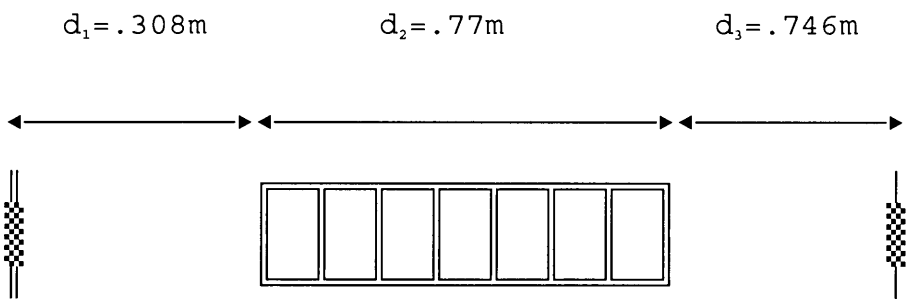

Figure 21 Total TOF of the cooled atoms. t_1, t_2, and t_3 correspond to the TOF in different regions where the atoms move with different velocities.

Table VI shows the TOF of the cooled atoms and the approximate channels around which the cooled atoms should appear for different detunings (different final velocities).

δ (MHz)	V_f (m/s)	V_i (m/s)	TOF (ms)	Channel
100	81	560	11.10	277
200	162	578	6.77	169
300	243	606	5.14	128
400	325	643	4.18	104
500	406	687	3.59	89
600	487	738	3.1	77

Table VI. δ is the laser detuning; v_f is the final velocity corresponding to the detuning δ, v_i is the initial velocity that could be cooled (for B_o given in Table III); TOF is the total time of flight and the channel gives the centered position of the cooled atoms' distribution (TOF=Ch.x40 μsec).

Figures 22-24 show the TOF distribution of metastable atoms corresponding to a sequence of different detunings (different final velocities) with the same tapered magnetic field (TMF) where B_o=170 Gauss. This initial magnetic field guarantees that the total change of the magnetic field in the 77cm will allow $(dB/dz) < (dB/dz)_{max}$. The currents used to create the magnetic profile are: .4A, .35A, .3A, .25A, .2A, .15A, .08A. Solid lines show the

centered channel of the cooled atoms' distribution. The initial velocity V_i was calculated by: $V_i=B_o/.879+V_f$. The results are summarized in Table VII. To achieve lower velocities one simply tunes the laser to be initially in resonance with slower atoms (less detuning).

δ MHz	V_f m/s	V_i m/s	TOF_cms	$Chann_c$	TOF_mms	$Chann_m$
300	243	436	5.86	146	5.64	141
350	285	477	5.15	130	5.04	126
400	325	518	4.6	115	4.16	104

Table VII. δ is the laser detuning; v_f is the final velocity corresponding to the detuning δ, v_i is the initial velocity that could be cooled for given B_o; TOF_c is the calculated total time of flight (See Fig. 21) and the channel gives the centered position of the cooled atoms' distribution (TOF=Ch.x40 μsec); TOF_m is the measured TOF from the channel where the distribution of the cooled atoms is centered.

As seen from Figs. 22-24, the full width at the half maximum (FWHM) of the cooled velocity distribution ΔV (relative to the central velocity) decreases as the final velocity is lowered. Deceleration and velocity bunching of atoms to a final velocity that depend on the detuning of the laser relative to a frequency of the transition have been observed. For final velocities of about 240m/s, the width Δv

of the cooled atoms peak is less than $v_f/15$ and the density of decelerated atoms (density per channel, or per velocity interval) is about 10 times that in the thermal beam distribution. Atoms with velocity 240m/s in the thermal distribution are in the background level (See Fig. 8, channel 190).

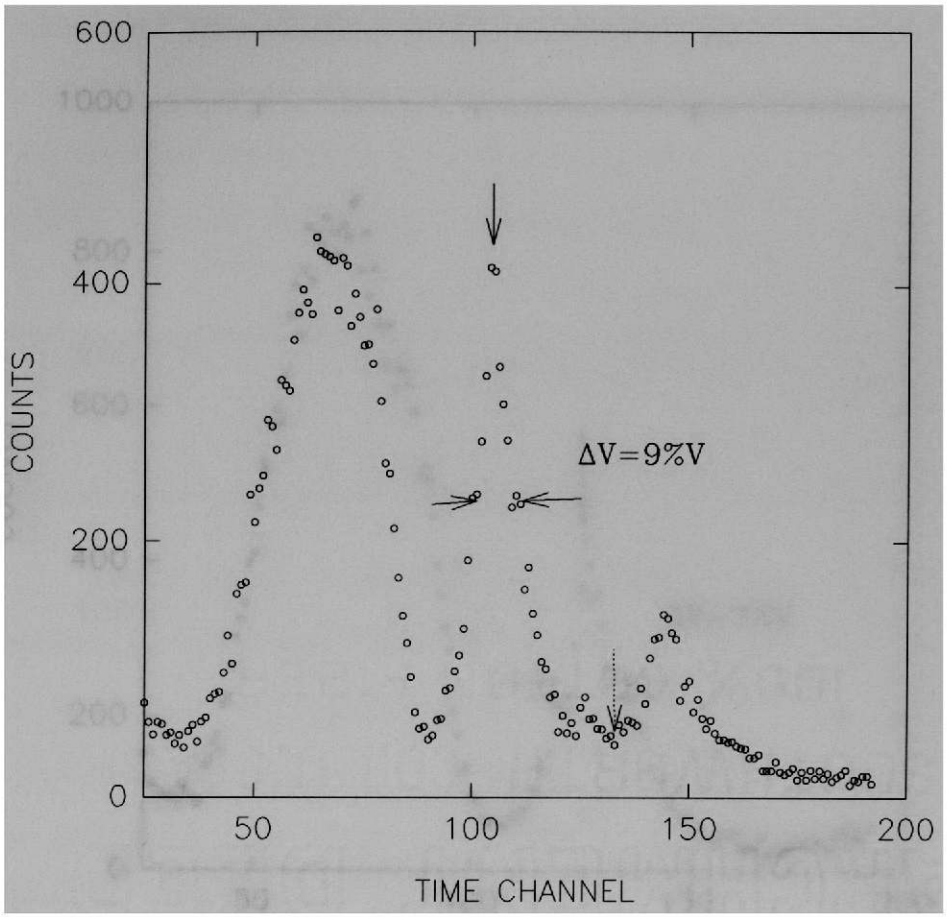

Figure 22 TOF Distribution of metastable atoms when the laser is detuned 400 MHz Red from resonance and a tapered magnetic field with B_o=170 Gauss is used.
The solid line shows the centered channel of the distribution of the tuned atoms.
TOF=4.16ms

Dashed line= lasers position

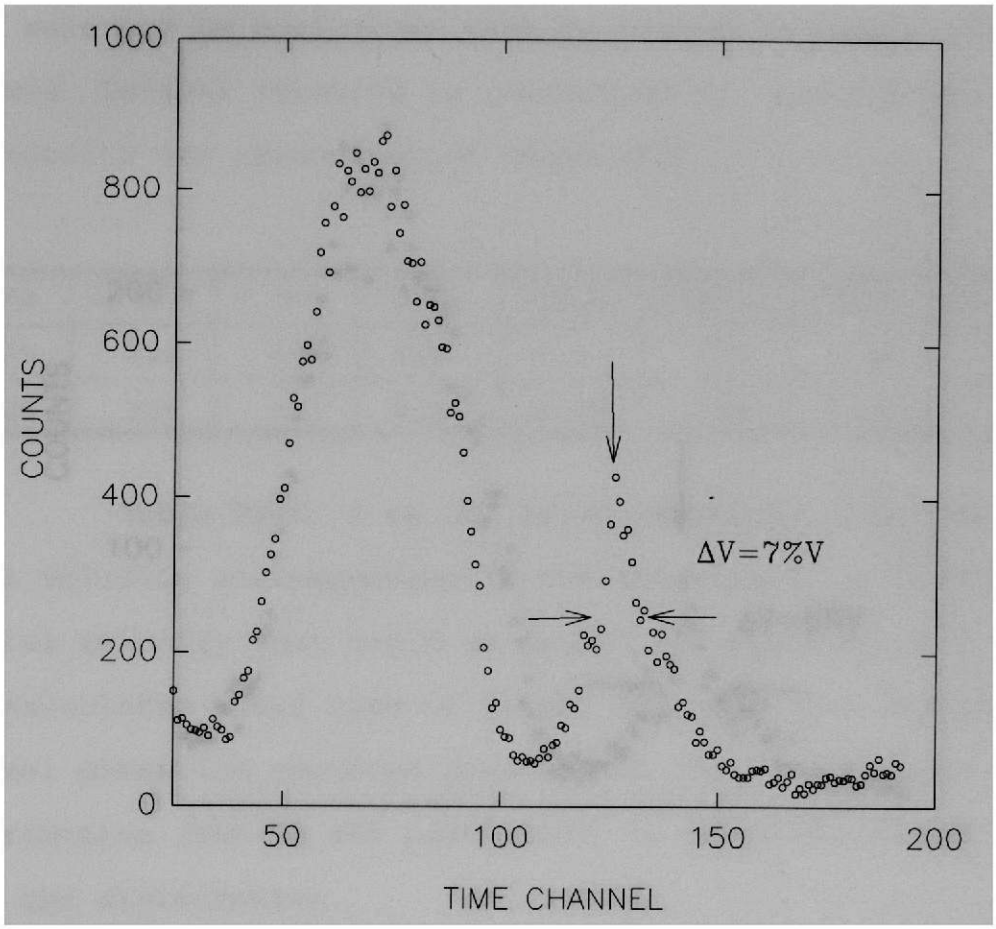

Figure 23 TOF Distribution of metastable atoms when the laser is detuned 350 MHz Red from resonance TMF with an initial magnetic field 170 Gauss. TOF=5.04ms

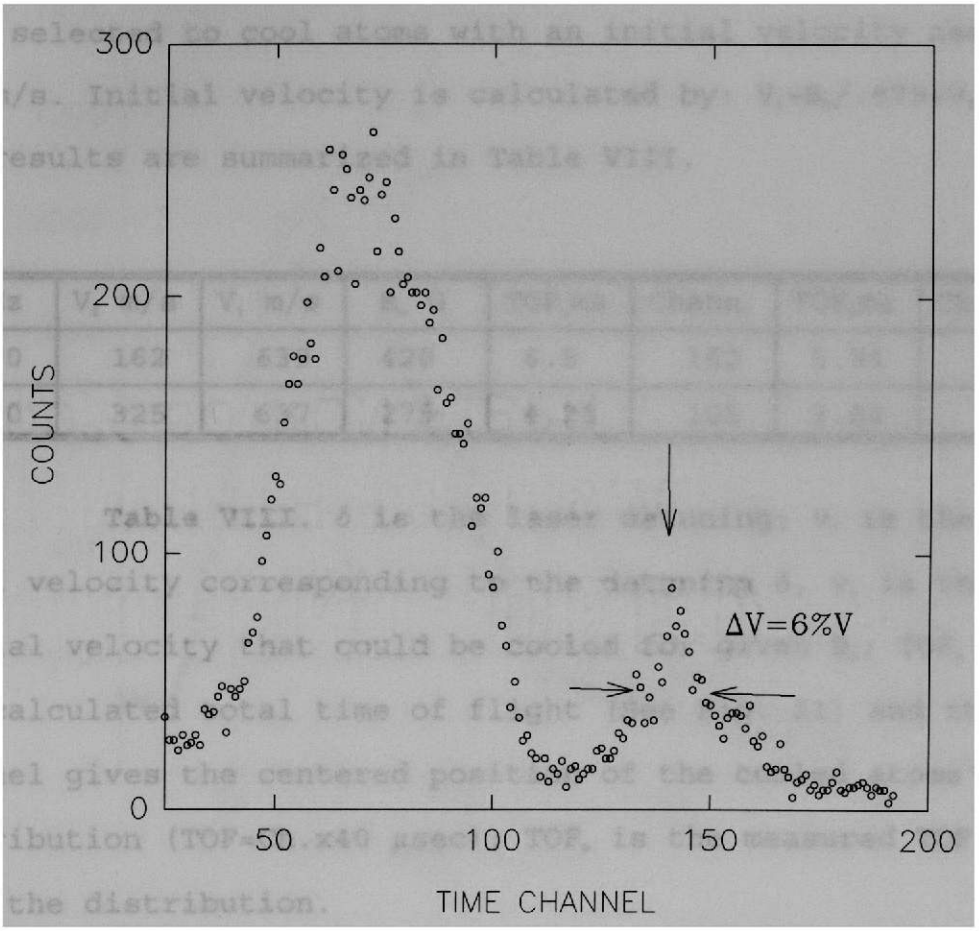

Figure 24 TOF Distribution of metastable atoms when the laser is detuned 300 MHz Red from resonance and a TMF with B_o=170 Gauss is used.

TOF=5.64 ms

Figures 25 and 26 show TOF distributions with and without the laser for different detunings and different tapered magnetic fields. Solid lines show the positions of the cooled atoms (channel where the distribution is centered). The detunings and the initial magnetic fields were selected to cool atoms with an initial velocity near 640 m/s. Initial velocity is calculated by: $V_i=B_o/.879+V_f$. The results are summarized in Table VIII.

δ MHz	V_f m/s	V_i m/s	B_o G	TOF_cms	$Chann_c$	TOF_mms	$Chann_m$
200	162	639	420	6.5	162	5.94	149
400	325	637	275	4.22	105	3.84	96

Table VIII. δ is the laser detuning; v_f is the final velocity corresponding to the detuning δ, v_i is the initial velocity that could be cooled for given B_o; TOF_c is the calculated total time of flight (See Fig. 21) and the channel gives the centered position of the cooled atoms' distribution (TOF=Ch.x40 μsec); TOF_m is the measured TOF from the distribution.

In this case, the FWHM of the cooled velocity distribution ΔV, relative to the central velocity v_f, decreases as the final velocity is lowered, but is higher in comparison with the case when the tapered magnetic field has lower initial value (compare Figures 24 and 26).

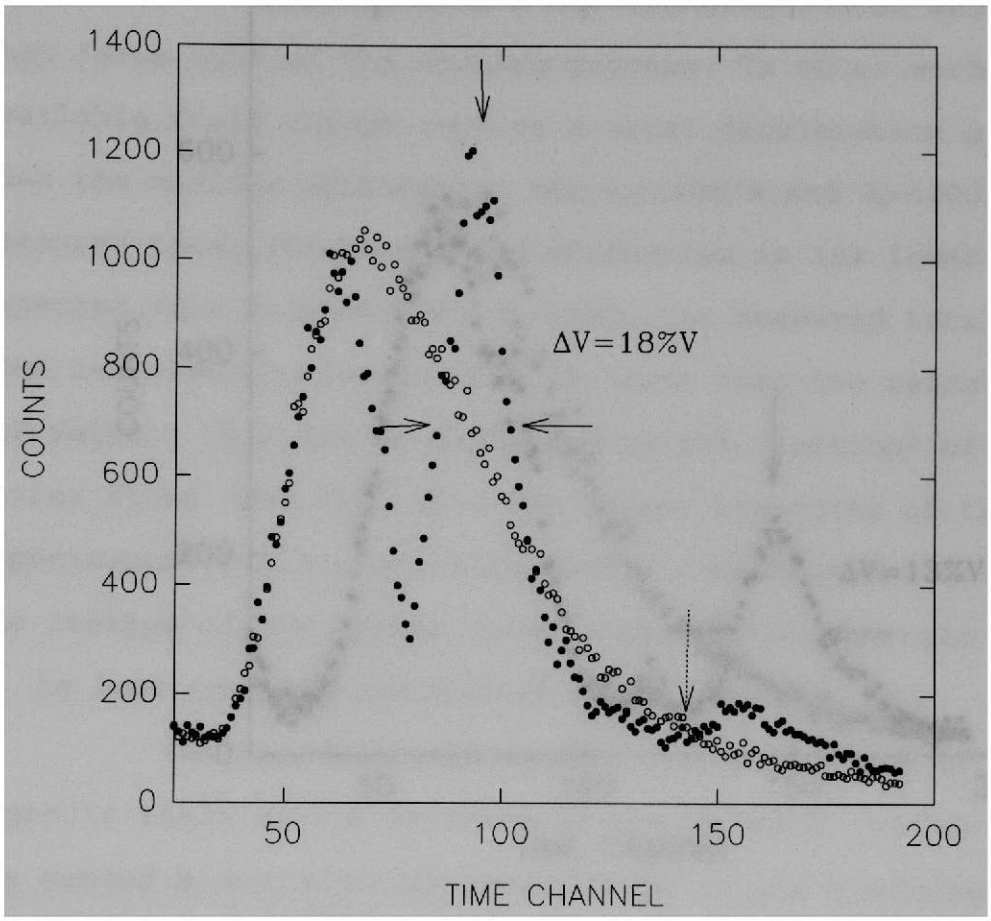

Figure 25 Hollow circles – TOF Distribution of the metastable atoms without the laser.

Filled circles – TOF Distribution when the laser is detuned 400 MHz Red from resonance, and tapered magnetic field (TMF) with currents .72, .50, .48, .42, .35, .3, .23 A is used. Initial magnetic field 275 Gauss.

Total TOF=3.84ms

⋯⋯> Position of the laser.

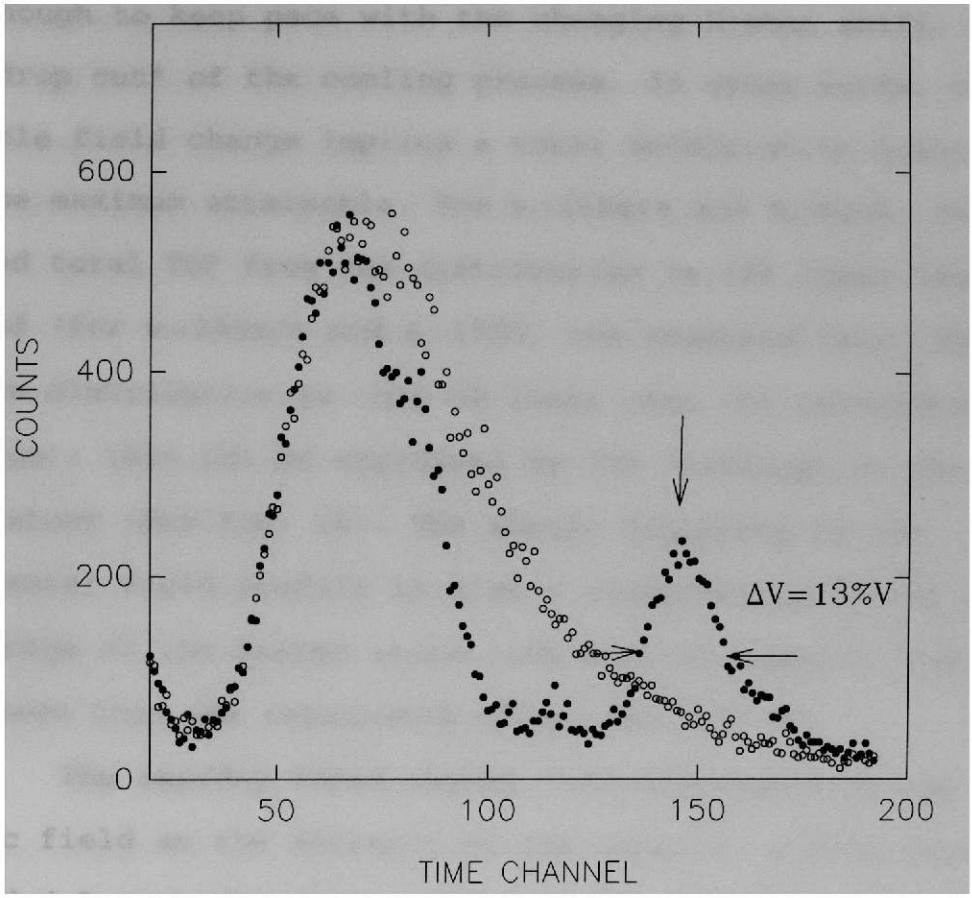

Figure 26 Hollow circles – TOF Distribution of the metastable atoms without the laser.
Filled circles – TOF Distribution when the laser is detuned 200 MHz Red from resonance, and TMF with the currents 1.1, .7, .67, .61, .58, .43, .3 is used. Initial magnetic field 420 Gauss.
Total TOF=5.94ms

It is because the field, for the case shown in Fig. 26, changes so rapidly, $(dB/dz) \rangle (dB/dz)_{max}$, that the rate of Zeeman shift change exceeds the possible rate of Doppler shift change. The faster atoms cannot decelerate fast enough to keep pace with the changing Zeeman shift, and they "drop out" of the cooling process. In other words, the available field change implies a total deceleration greater than the maximum attainable. For v_f=160m/s and B_o=420G, the measured total TOF from the distribution is 10% lower than expected (for v_f=240m/s and B_o=170G, the measured total TOF from the distribution is only 3% lower than the calculated TOF value); this can be explained by the "leaking" of the faster atoms (See Fig. 26). The abrupt beginning of the experimental field profile is also a contributing factor to the leakage of the faster atoms (the initial magnetic field, B_o, is less than the calculated value, See Fig. 5).

The rapidly field change, the difference of the magnetic field an the entrance of the magnetic system from the needed B_o and also the uncertainty in the zero laser detuning explain why the TOF distribution in the case of δ=0 and the TMF with B_o=490 Gauss (Fig.19) is "attenuated" in the channel corresponding to an initial velocity about 420m/s and not 550m/s for which the spatially varying field was calculated.

CHAPTER VI - CONCLUSIONS

In this thesis, the laser cooling of a metastable, thermal-argon beam was successfully demonstrated using the momentum transfer from a counterpropagating laser beam and the Zeeman cooling approach to compensate for the changing Doppler shift that takes the atoms out of resonance during the cooling process. The atomic velocity distribution was determined by the TOF spectroscopy. This technique depends only on the absolute measurement of the time of flight of the atoms along a known path; and for low velocities, gives a velocity resolution few times better than other used techniques, for example observation of the fluorescence induced by a second, very weak probe laser which crosses the atomic beam at a certain angle[32] (the natural width of the atomic cycling transition in the Argon $\gamma=1/2\pi\tau\sim5.3$MHz gives a velocity resolution $\Delta v=\lambda\gamma\sim4.5$m/s by this method).

One of the primary original motivations for the laser cooling, and a future step in this work, is the possibility of trapping neutral atoms in electromagnetic fields (Magneto-Optical Trap). The basic problem is that most such traps are so shallow in energy that very slow atoms are required.

The use of a longer spatially varying field, and consequently, the possibility of a larger field change, will allow a larger velocity reduction while keeping the rate of change of the field small enough that the atoms can stay in

resonance as they decelerate. This will produce, in addition to deceleration and cooling to a final velocity very close to zero, a compression of the velocity distribution of the cooled atoms. The production of very slow, cold atomic beam, with velocity spread less than 6% and a high density of atoms, demonstrates the utility of laser deceleration for atomic-beam "velocity selection". The advantage of this laser velocity selection over mechanical selection is that unwanted velocities are compressed into the desired velocity rather than being discarded.

The ability to produce high intensity, nearly monoenergetic atomic beams as in Figures 22-24 raises the possibility of many interesting atomic beam experiments. Experiments with trapped and laser cooled atoms will improve the resolution in ultra-accuracy spectroscopy, the frequency standards and many experiments in fundamental physics.

We are continuing to work on improving the polarization of the laser beam; focusing the cooling laser at the exit of the metastable argon source (this convergence leads to a reduction of the atoms' transverse momentum, thus reducing the increase in atomic beam divergence as the longitudinal velocity decreases); reducing the laser drift and the error during the laser tuning process. We are also working on new magnets to increase the length of the magnet system and we have already constructed the coils for a quadrupole trap[33] and the trapping chamber.

LIST OF REFERENCES

1. J. Michael Hollas, High Resolution Spectroscopy, Butterworths, 8.2.8 Saturation Spectroscopy.

2. Bordé,C.J. Compt. rend.,271B,371 (1970).

3. Smith,P.W. and Hänsch,T.W. Phys. Rev. Lett.,**26**,29 (1971).

4. Sorem,M.S. and Schawlow,A.L.(1972). Optics Commun.,**5**,148

5. Wieman,C. and Hänsch,T.W.(1976) Phys.Rev.Lett.,**36**,1170.

6. P.C.Engelking,Rev.Sci.Instrum.**57**, 2274 (1986)

7. P.L.Gould,G.A.Ruff,D.E.Pritchard,ibid.**56**, 827 (1986).

8. R.Cook,Opt.Commun.**35**, 347 (1981).

9. M.A.Bouchiat and L.Pottier,Science **234**, 1203 (1986).

10. A. Einstein, Sitzungsber.Kgl.Preuss.Akad.Wiss.1924 261 (1924).

11. S.N.Bose, Z. Phys.**26**, 178 (1924).

12. M.H.Anderson, J.R.Ensher, M.R.Matthews, C.E.Wieman, E.A.Cornell. Science ,Vol. **269**, 14 July 1995.

13. C.C.Bradley, C.A.Sackett, J.J.Tollet, and R.G. Hulet. Phys. Rev. Lett., Vol 75, 9, 1687, 28 August 1995.

14. K.B.Davis, M.O. Mewes,M.R. Andrews,N.J. van Druten, W. Ketterle,et al.,Phys.Rev.Lett.,Vol 75, 22,3969, 27 Nov 1995.

15. D.J.Wineland and H.Dehmelt, Bull. Am. Phys. Soc., **20**, 637 (1975).

16. J.C.Bergquist, D.J.Wineland,et al., Phys. Rev. Lett. **55**, 1567 (1985).

17. D.J.Larson, J.C.Bergquist, D.J.Wineland,et al., Phys. Rev. Lett. **57**, 70 (1986).

18. P.W.Milonni, J.H.Eberly, Lasers,John Wiley & Sons, 1988.

19. V.S.Letokhov, V.G.Minogin et al., Opt.Commun., **19**, 72 (1976).

20. Phillips, W.D, John V.Prodan and Harold J. Metcalf. Journal of the Opt. Soc. of America B, **2**, 1751, Nov,1985.

21. D.A.Landman, Phys. Rev.,173,33 (1968).

22. Atomic Energy Levels, C.E.Moore, NSRDS-NBS35, Vol I,211.

23. Second Interim Technical Report. Federal Demostration, Project F49620-93-1-0159DEF. FIU, Miami, Fl, 15 March 1995.

24. K.B.MacAdam, C.Wieman, A.Steinbach. Am.J.Phys., **60**, 12, (1992).

25. C. Avila, G.B.Ramos, J.W.Sheldon, K.A. Hardy, et al., Abstract published in Bull. Am. Phys. Soc., **40**, 2072 (1995).

26. Coherent 899-21, Operator's Manual.

27. A. Barrios, et al.,J. Appl. Phys.,76(2),15 July 1994.

28. G.B.Ramos,et al.,Phys. Review A, Vol 51, 4, April. 1995.

29. K.Hardy and J.W.Sheldon, Rev.Sci.Instrum.,**52**,1802(1981).

30. K.A. Hardy, et al., J. Appl. Phys., **67**, 7240 (1990).

31. A. Barrios, K.A. Hardy, J.W. Sheldon and J.R. Peterson, Phys. Rev. Lett. **69**, 1348 (1992).

32. Phillips, W.D, John V.Prodan and Harold J. Metcalf. Prog. Quant. Electr. 1984 Vol. 8 pp 119-127. Printed in Great Britain.

33. Harold Metcalf, Atomic Cooling And Trapping. Encyclopedia of Applied Physics, Vol.2, 1991 VCH Publishers, Inc.

APPENDIX

LIST OF ABSTRACTS

Dissociative Recombination (DR) Studies of He_2^+ and Other Rare Gas Molecular Ions. C.Avila, G.B.Ramos, L.Simons, J.W.Sheldon and K.A.Hardy, Florida International University, J.W.Peterson, SRI International & Florida International University. Presented at the Southeastern Section of the American Physical Society, Tallahassee, Fl. November 1995. Abstract published in Bull. Am. Phys. Soc., **40**, 2071 (1995).

Velocity Hole Burning in Argon as a Precursor to Laser Cooling. C.Avila, G.B.Ramos, L.Simons, A.Farnsworth, J.W.Sheldon and K.A.Hardy, Florida International University. Presented at the Southeastern Section of the American Physical Society, Tallahassee, Fl. November 1995. Abstract published in Bull. Am. Phys. Soc., **40**, 2072 (1995).

Time-of-flight (TOF) Measurements of the Laser Cooled Metastable Argon Atomic Beam. C.A.Avila, G.Hernandez, J.W. Sheldon and K.A.Hardy, Florida International University. Submitted for publication.